

國立交通大學

電控工程研究所

碩士論文

RSA 分析應用於禪坐心肺交互作用之研究

Investigation of Chan-meditation Cardiorespiratory
interaction by RSA analysis

研究生：楊淮璋

指導教授：羅佩禎 博士

中華民國九十九年七月

RSA 分析應用於禪坐心肺交互作用之研究
Investigation of Chan-meditation Cardiorespiratory
Interaction by RSA Analysis

研究生：楊淮璋

Student: Hwan Jang Yang

指導教授：羅佩禎 博士

Advisor: Dr. Pei-Chen Lo

國立交通大學

電控工程研究所

碩士論文

A Thesis

Submitted to Institute of Electrical and Control Engineering
College of Electrical Engineering National Chiao Tung University

In Partial Fulfillment of the Requirements

For the Degree of

Master

In

Electrical and Control Engineering

July 2010

Hsinchu, Taiwan, Republic of China

中華民國九十九年七月

RSA 分析應用於禪坐心肺交互作用之研究

研究生：楊淮璋

指導教授：羅佩禎 博士

國立交通大學電控工程研究所



本研究的目的是在於藉著量化呼吸性竇性心律不整(Respiratory sinus arrhythmia)探討呼吸調控下與禪坐調息時的心肺交互作用。呼吸性竇性心律不整之量化，多用於探討副交感神經活躍的程度或是心肺氣體交換的效率。本研究共收集了 12 位年齡相似的受測者的心電圖和呼吸訊號，其中實驗組為 6 位具有禪坐經驗者，而控制組 6 位受測者則無此經驗。由結果發現，控制組在控制呼吸速率較慢(每分鐘六次呼吸)的情況下，呼吸性竇性心律不整(RSA)值都有顯著增加(p 值皆小於 0.05)。根據此結果，禪坐時在呼吸速率較慢下，呼吸性竇性心律不整(RSA)值並無明顯地增加。關於探討呼吸性竇性心律不整(RSA)值和呼吸速率負相關性的結果，我們個別觀察控制呼吸是顯著負相關 (p 值小於 0.05)，但禪坐組並無此顯著現象，禪坐組中相關性的不確定性，可能是由於其他生物或意識因素冥想所干預。

Investigation of Chan-meditation Cardiorespiratory Interaction by RSA Analysis

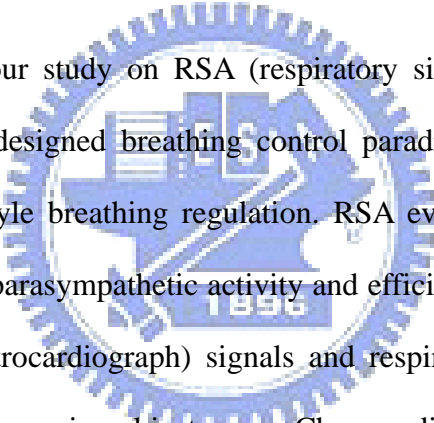
Student : Hwan Jang Yang

Advisor : Dr. Pei-Chen Lo

Institute of Electrical and Control Engineering

National Chiao Tung University

Abstract



This thesis reports our study on RSA (respiratory sinus arrhythmia) analysis for the control group under pre-designed breathing control paradigm and the experimental group under Chan-meditation style breathing regulation. RSA evaluation has been applied to the investigation of levels of parasympathetic activity and efficiency of pulmonary gas exchange. In this study, ECG (electrocardiograph) signals and respiratory signals of twelve subjects were recorded. Among them, six subjects were Chan-meditation practitioners and the other six subjects are normal people in the same age range, yet, without any meditation experience.

As a brief summary of our preliminary results, control subjects under slow breathing (breathing control at rate 6 breaths/min) exhibited the enhanced RSA rate ($p < 0.05$), while the experimental subjects did not. In regards to the study on correlation between RSA rate and respiratory rate, we observed the significant negative correlation in control group ($p < 0.05$). Nevertheless, relationships disclosed in experimental group involved uncertainties that might be due to the intervention of other biological/conscious factors in meditation.

誌 謝

轉眼間已完成口試，由於服完兵役後，在因緣際會下有幸得以繼續進修，深感機會之不易，步入社會前的讀書生涯自當珍惜。先感謝電控所的教授們有這麼多豐富的課程得以修習，令我在專業知識上獲益良多。

家人是我最重要的貴人—爸、媽和妹妹，可以持續求學，都是因為你們的支持和體諒，你們是我最大的靠山。

我的指導教授—羅佩禎博士，感謝您在學術研究上的身教、言教。因為您的指導，我的碩士生涯才能有如此充實、多元的歷練。

研究路上的戰友們—，順敏、盧兄、宣竹、仁宏、明誠、翔宇、介均謝謝有你們一起吃飯、聊天、打球、討論研究，因為有你們，實驗室總是充滿歡樂。

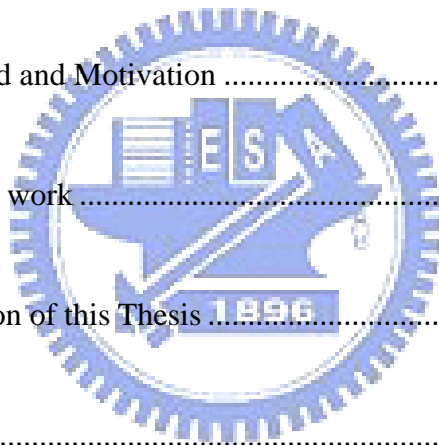
最後，感謝口試委員—張剛鳴教授、林國瑞教授，有您們的指導，我的碩士論文才能更臻完備。



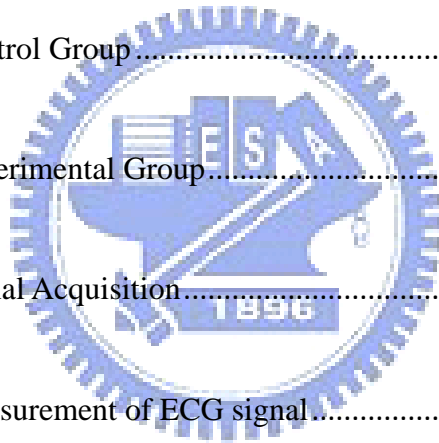
淮璋 庚寅 於交通大學

Contents

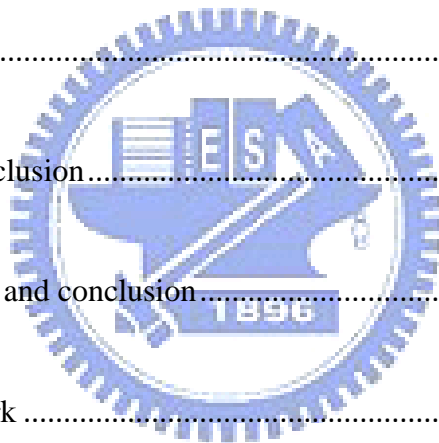
Contents	i
List of Figure.....	v
List of Table	viii
Chapter1	1
Introduction.....	1
1.1 Background and Motivation	1
1.2 Aim of this work	3
1.3 Organization of this Thesis	4
Chapter 2.....	5
Theories and Methods.....	5
2.1 Introduction to ECG and Respiration	6
2.1.1 Introduction to ECG.....	6
2.1.2 Chest and Abdominal Respiration	9
2.2 Evaluation of Respiratory Sinus Arrhythmia (RSA)	11



2.2.1 Introduction to RSA	11
2.2 Evaluation of RSA	13
2.3 Correlation coefficient	14
Chapter 3	16
Experiment and Signal Analysis	16
3.1 Experimental Setup and Procedure	16
3.1.1 Control Group	17
3.1.2 Experimental Group	17
3.1.3 Signal Acquisition	18
3.1.4 Measurement of ECG signal	20
3.1.5 Measurement of respiratory signal	21
3.2 Strategy for RSA Quantification	22
Step 1 Pre-processing	23
Step 2 RSA quantification	23
3.3 Statistical Evaluation	26



Chapter 4.....	29
Experimental Results And Analysis.....	29
4.1 Results of RSA analysis.....	29
4.2 RSA rate and respiratory rate.....	37
4.2.1 Results for individual subject.....	38
4.2.2 Results for entire group.....	49
Chapter 5.....	53
Discussion and conclusion.....	53
5.1 Discussion and conclusion.....	53
5.2 Future Work.....	54
Reference	55
Appendix A	59
R Peak and Respiratory Peak Detections.....	59
A.1 R Peak Detection.....	59
A.2 Respiratory Peak Detection.....	61

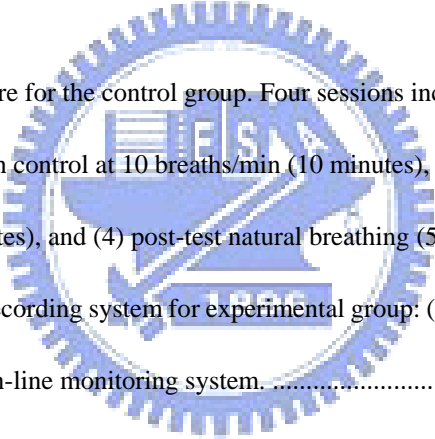


Appendix B64

Formal Chan-meditation Practice64



List of Figure

Fig.2. 1 The conducting system of the human heart.	7
Fig.2. 2 The standard wave pattern of ECG	8
Fig.2. 3 Illustration of expiration and inspiration mechanisms in chest respiration	10
Fig.2. 4 Illustration of expiration and inspiration mechanisms in abdominal breathing.....	10
Fig.2. 5 RSA phenomenon illustrated by the increase (decrease) of heart rate during inspiration (expiration).....	12
	
Fig.3. 1 Experimental procedure for the control group. Four sessions include (1) baseline measurement (5 minutes), (2) breath control at 10 breaths/min (10 minutes), (3) breath control at 6 breaths/min (10 minutes), and (4) post-test natural breathing (5 minutes).....	17
Fig.3. 3 Physiological signal recording system for experimental group: (a) Bluetooth Bio-amplifiers, and (b) digitization and on-line monitoring system.	19
Fig.3. 2 Physiological signal recording system for control group: (a) Bio-amplifiers, and (b) digitization and on-line monitoring system.	19
Fig.3. 4 (a) ECG electrode, (b) Bipolar limb-lead II electrode placement(experimental group) and (c) Bipolar limb-lead I electrode placement(control group).	20
Fig.3. 5 Piezo-electric respiratory transducer.	21
Fig.3. 6 Respiratory signal.....	22
Fig.3. 7 Signal flow graph for RSA quantification.	24
Fig.3. 8 (a) This example uses five respiratory cycles as a window to calculate RSA rate. (b) Based on a window size of five respiratory cycles, we may find five local maximum points of RR_i . (c) Based on a window size of five respiratory cycles, we may find five local minimum points of	

RR _j	25
Fig.3. 9 Sequences of RRI, heart rate, RSA rate and respiratory rate, from the top. In (I) and (IV) sessions, the subject breathed normally at their natural breathing rate. In (II) and (III) sessions, the subject followed an auditory-cue guidance to breathe at the rate of respectively 10 and 6 breaths per minute.	26
Fig.3. 10 Signal flow graph of evaluating correlation coefficients between respiratory rate and RSA rate in the slow, medium, and fast HR range.....	28
Fig.4. 1.(a)Time-dependent RSA rates for experimental subject 1 (a)-(f) show the results for subject 1-6 respectively.....	33
Fig.4. 2 Average and standard deviation of RSA values in Session II and Session III. From (a) to (f), results of six control subjects all demonstrate the increase from Session II to III.	36
Fig.4. 3 RSA rate versus RR in the fast HR range for control subject 1-6 (from (a) to (f))......	39
Fig.4. 4 RSA rate versus RR in the medium HR range for control subject 1-6 (from (a) to (f)).....	40
Fig.4. 5 RSA rate versus RR in the slow HR range for control subject 1-6 (from (a) to (f)).	41
Fig.4. 6 RSA rate versus RR in the fast HR range for experimental subject 1-6 (from (a) to (f)) during the first meditation session.	42
Fig.4. 7 RSA rate versus RR in the medium HR range for experimental subject 1-6 (from (a) to (f)) during the first meditation session.....	43
Fig.4. 8 RSA rate versus RR in the slow HR range for experimental subject 1-6 (from (a) to (f)) during the first meditation session.	44
Fig.4. 9 RSA rate versus RR in the fast HR range for experimental subject 1-6 (from (a) to (f)) during the second meditation session.	45
Fig.4. 10 RSA rate versus RR in the medium HR range for experimental subject 1-6 (from (a) to (f))	

during the second meditation session.	46
Fig.4. 11 RSA rate versus RR in the slow HR range for experimental subject 1-6 (from (a) to (f)) during the second meditation session.	47
Fig.4. 12 Correlation coefficients of each individual control subject in the fast, medium and slow HR range.	48
Fig.4. 13 Correlation coefficients of each individual experimental subject in the fast, medium and slow HR range during the first meditation session.....	48
Fig.4. 14 Correlation coefficients of each individual experimental subject in the fast, medium and slow HR range during the second meditation session.....	48
Fig.4. 15 Correlation analysis for RSA rate and RR based on the entire aggregating group data. Results of control group are plotted in (a) fast HR, (c) medium HR, and (e) slow HR. Results of experimental group are shown in (b) fast HR, (d) medium HR, and (f) slow HR.	51
Fig.4. 16 Piecewise linear fitting: (control) 5-10 and 10-20 breaths/min for both fast and slow HR; 5-10, 10-15, and 15-20 breaths/min for medium HR.(experimental) 8-10 and 10-18 breaths/min for fast HR, 8-10,10-16, and 16-18 breaths/min for medium HR, 9-17 breaths/min for slow HR.....	52
Fig.A. 1 Flow chart of R peak detection.....	60
Fig.A. 2 ECG after preprocessing	61
Fig.A. 3 Flow chart of Respiratory peak detection.....	62
Fig.A. 4 Respiratory signal after preprocessing	63
Fig.A. 5 The parameters of respiratory signal	63

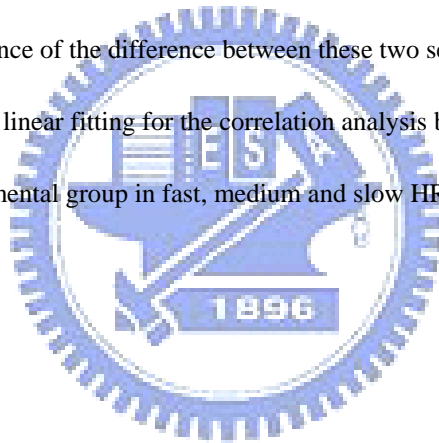
List of Table

Table.2. 1 Described each ECG complex correlates to the particular task of the cardiac cycle.8

Table.3. 1 Subjects of experimental and control groups16

Table.4. 1 Average and standard deviation of RSA values for 6 control subjects in Sessions II and III.
Statistical significance of the difference between these two sessions is apparent ($p < 0.05$)...37

Table.4. 2 Multiple piecewise linear fitting for the correlation analysis between RSA rate and RR for
control and experimental group in fast, medium and slow HR.....50

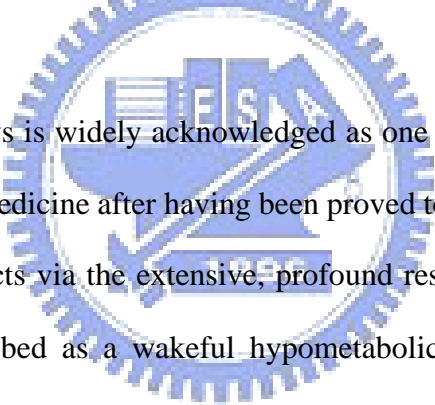


Chapter1

Introduction

Chapter 1 contains three major sections. Section 1.1 briefly introduces the background and motivation of this study. Section 1.2 brings in the aim of this study. Finally, the organization of this thesis is described in Section 1.3.

1.1 Background and Motivation



Meditation nowadays is widely acknowledged as one important technique in the category of mind-body medicine after having been proved to benefit human health and wellness in various aspects via the extensive, profound researches since 1960s[1][2] and Meditation is described as a wakeful hypometabolic state of parasympathetic dominance that has been corroborated by such physiological indicators as the reduction of heart rate, blood pressure, and respiratory rate, significant increase in plasma melatonin levels and better regulation of cortisol level[3][4][5]. Among various meditation techniques, Chan meditation originating from Dharma-Chan reveals an extraordinarily unique way of practicing meditation via “holy-heart unification” enlightenment. Our previous study on EEG (electroencephalograph) has revealed some exclusive characteristics of a Chan-enlightened brain[6][7]. Nevertheless, the core doctrine in Dharma Chan focuses a great deal on the practice of *heart* purification that has been assumed to power the Chan-enlightened brain (Appendix B). Mechanism of heart purification involves both Chan wisdom practice and heart-chakra purification.

Chan-meditation practitioners thus have been experiencing various evolutionary states of heart perception that inspires us to investigate the cardiac physiology during Chan meditation. To the best of our knowledge, no study has been reported on the cardiorespiratory interaction during Chan-meditation practice because orthodox Dharma-Chan practice is rarely found in the current era.

The interaction between human cardiac and respiratory systems has been widely studied for many decades. It has been disclosed that these two systems do not act independently; instead, they are coupled by some mechanisms. One well-known phenomenon of cardiorespiratory interaction is the frequency modulation of heart rate by respiration, which is known as respiratory sinus arrhythmia (RSA)[8]. RSA actually portrays the heart rate variability (HRV) in synchrony with respiration in the sense that heart rate increases during inspiration and decreases during expiration. RSA mechanism facilitates the efficiency of human pulmonary air exchange[9].

Previous studies have shown that the efficiency of pulmonary gas exchange is improved by RSA, suggesting that RSA may play an active physiologic role[10][11]. The matched timing of alveolar ventilation and its perfusion with RSA within each respiratory cycle could save energy expenditure by suppressing unnecessary heartbeats during expiration and ineffective ventilation during the ebb of perfusion. Furthermore, evidence has accumulated of a possible dissociation between RSA and vagal control of that heart rate, suggesting differential controls between the respiratory modulation of cardiac vagal outflow and cardiac vagal tone. RSA or heart rate variability in synchrony with respiration is a biological phenomenon, which may have a positive influence on gas exchange at the level of the lung via efficient ventilation/perfusion matching[12].

The living manner nowadays tends to create stress in varying degrees and forms for modern people, that unfortunately inhibits parasympathetic activity. Meditation practice has become one of the most popular stress-relief approaches. The mechanism of stress management via Dharma-Chan meditation (Appendix B) involves multi-faceted phases, for instance, bioenergy enhancement via harmonizing with Chan supreme life power and life-scope expansion via Chan wisdom enlightenment. RSA has been acknowledged as a reliable indicator for parasympathetic efferent activity. Moreover, RSA can be assessed quantitatively by simultaneously recording ECG (electrocardiograph) and respiratory signals.

RSA characterized by such particular heart rate oscillations appears to be similar to HRV patterns reported for practitioners of Chinese Chi, yogic, and Zen traditions[11][13]. This finding arouses our attention of investigating the hypothesis: Chan meditation with major focus on heart-purification practice may effectively induce prominent RSA. Moreover, belly breathing might be another mechanism of arousing RSA. There leave a number of interesting topics valuable for further study.

1.2 Aim of this work

This study was aimed at the investigation of RSA behaviors under breathing control (control group) and Chan meditation (experimental group). Quantitative approach for evaluating RSA rate was applied to the RRI (R-to-R interval) sequence. In addition, correlation analysis was conducted to disclose the relationship between RSA rate and respiratory rate.

1.3 Organization of this Thesis

This thesis is composed of five chapters. Chapter 1 introduces the background, motivation, and main aim of this study. Chapter 2 briefly describe ECG and respiratory signal, theory and methods for RSA Quantification and statistical analysis. In Chapter 3, the experimental setup and protocol are presented. Then the strategies for RSA quantification and correlation coefficient analysis are illustrated. Chapter 4 reports and discusses the results. The last chapter makes a summary of this research and brings forward some issues for future study.



Chapter 2

Theories and Methods

According to Chan-Meditation practitioners, perceived benefits to health have been confirmed in the physiological, psychological, behavioral, and mental aspects. Researchers accordingly intended to investigate the phenomena of meditation as early as in the 1950's. Scientific evidences based on measurable, empirical data have been reported at an increasing rate, thanks to the fast development of sophisticated medical instruments that provide the media for gaining access to physiological signals. Nevertheless, we hardly found any report of the effects of Chan-meditation practice on cardio-respiratory interaction that has been identified as an important index of health condition and stress-management ability. The cardiorespiratory function now can be assessed quantitatively by simultaneously recording ECG (electrocardiograph) and respiratory signals.

Scientific researches have demonstrated that a number of physiological signals accessible noninvasively significantly reveal the normal/abnormal and physically/mentally health states of human body. They even have become routinely clinical reference or medical-checkup items due to the ease of implementation. Examples of these physiological signals include ERP (evoked-response potential), EMG (electromyograph), ECG, GSR (galvanic Skin Response), and respiratory signal. To investigate the interactions between cardiac and respiratory systems, background and fundamentals of ECG and respiratory signals are introduced in Section 2.1. Then,

Section 2.2 illustrates the theory and method of quantifying RSA experiment designed to analyze the parasympathetic activity by breathing control.

2.1 Introduction to ECG and Respiration

2.1.1 Introduction to ECG

As the core organ of the circulatory system, human heart pulsates automatically and rhythmically. Such mechanical activity is manipulated by a specialized conducting system composed of SA node (sinoatrial node), AV node (atrioventricular node), Bundle of His, and Purkinje fibers as shown in Fig.2.1. Pacemaker cells in SA node depolarize at the rate of approximately 72 times per minute to control the rhythmic pulsation of heart. The depolarization waves (action potential) spread out through the atria and propagate via the particular conduction pathways till reaching the cells of ventricles. When action potential travels to atria, atrial cells depolarize that causes the contraction of atria and results in the so-called P wave in ECG. After transmitting through AV node, Bundle of His, and Purkinje fibers (the extended part of the fibers of Bundle of His), action potential finally spreads to ventricular cells. The depolarization of ventricular cells causes the action of ventricular systole, which is recorded as the QRS wave (or simply R wave) in ECG. Then, T wave appears as the ventricular cells repolarize (ventricular diastole). Note that the wave of atrial repolarization is masked by the dominant QRS during ventricular depolarization. In sum, the electrical-conduction mechanism driving the atrial and ventricular, mechanical systole/diastole rhythms follows the sequence: SA node → atria → AV node → Bundle

of His → Purkinje fibers → ventricles[14].

The depolarization waves not only induce the mechanical pumping of heart but also generate the variation of electrical potential on the body surface that is recordable noninvasively. ECG is the signal revealing such electrical-potential change. Without stimulation, the heart cells are in the quiescent state (-80 mV or so) with negative potential (so-called polarization). After stimulation, they bear positive potential which induces the systole reaction. Hence, ECG traces the potential variation of periodic activity of the heart.

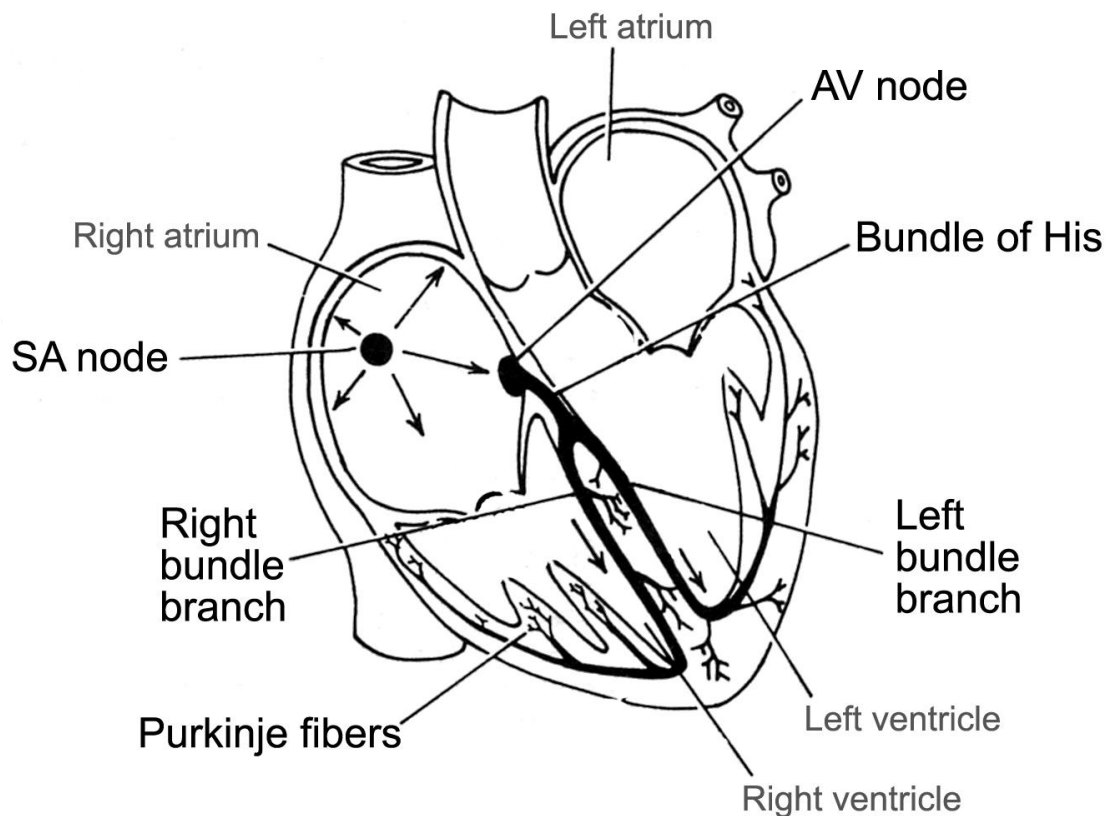


Fig.2. 1 The conducting system of the human heart. [14]

Table.2. 1 ECG complex corresponding to the electrical and mechanical actions in a cardiac cycle.

ECG pattern	Electrical activity	Mechanical activity
P wave	Depolarization of atrial cells	Atrial contraction
QRS complex	Depolarization of ventricular cells	Ventricular contraction
T wave	Repolarization of ventricular cells	Ventricular expansion

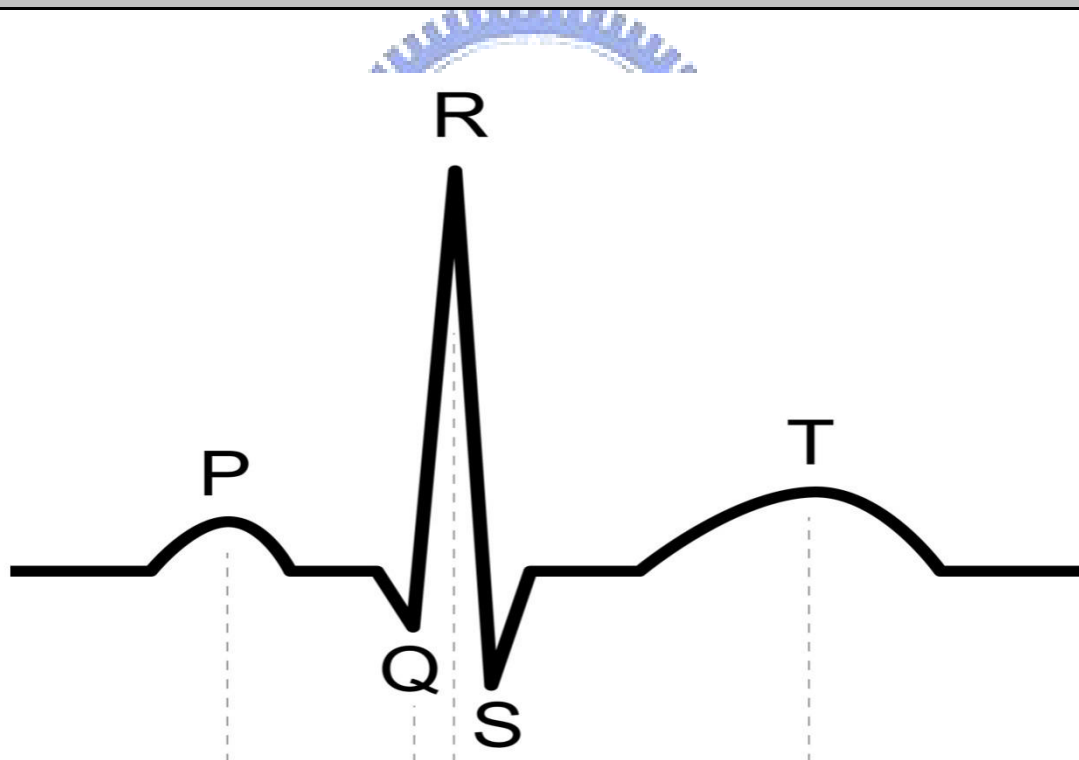
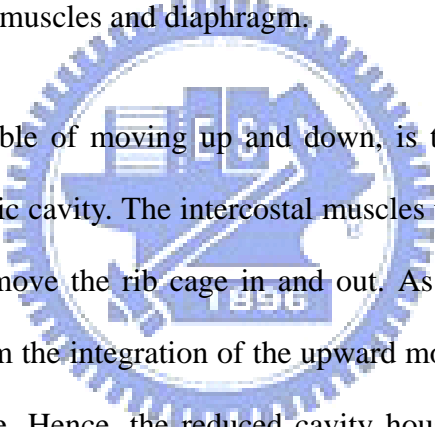


Fig.2. 2 The standard wave pattern of ECG

2.1.2 Chest and Abdominal Respiration

The respiration provides a means of acquiring oxygen and eliminating carbon dioxide for survival. The mechanism of respiration involves the muscular motions that change the volume of the thoracic cavity to achieve gas exchange by inspiration (inhalation) and expiration (exhalation). Normal, chest respiration is accomplished by two sets of muscles, the diaphragm and intercostal muscles. They operate together to carry out the task of inhalation/exhalation. On the other hand, abdominal respiration having been recognized to be a much healthier respiration manner is accomplished mainly by the abdominal muscles and diaphragm.



The diaphragm, capable of moving up and down, is the wall that separates the abdomen from the thoracic cavity. The intercostal muscles together with the ribs form the thoracic cavity and move the rib cage in and out. As shown in Fig.2.3, normal expiration is resulted from the integration of the upward motion of diaphragm and the inward swing of rib cage. Hence, the reduced cavity housing the lungs results in a pressure increase of -3mm Hg with respect to the pressure outside the body. Accordingly, air flows out of the lungs that completes the expiration scheme. On the contrary, inspiration follows the reverse mechanism.

In abdominal breathing, abdominal muscles expand causing the downward movement of diaphragm and, consequently the increase of thoracic-cavity volume inducing the air in (inspiration). While during the expiration, contraction of abdominal muscles moves diaphragm upward and narrow the thoracic-cavity volume that results in the air-out action. Instrumentation with appropriate transducer can be adopted to

record the respiration activities by transforming mechanical energy into electrical energy (for example, strain gauge).

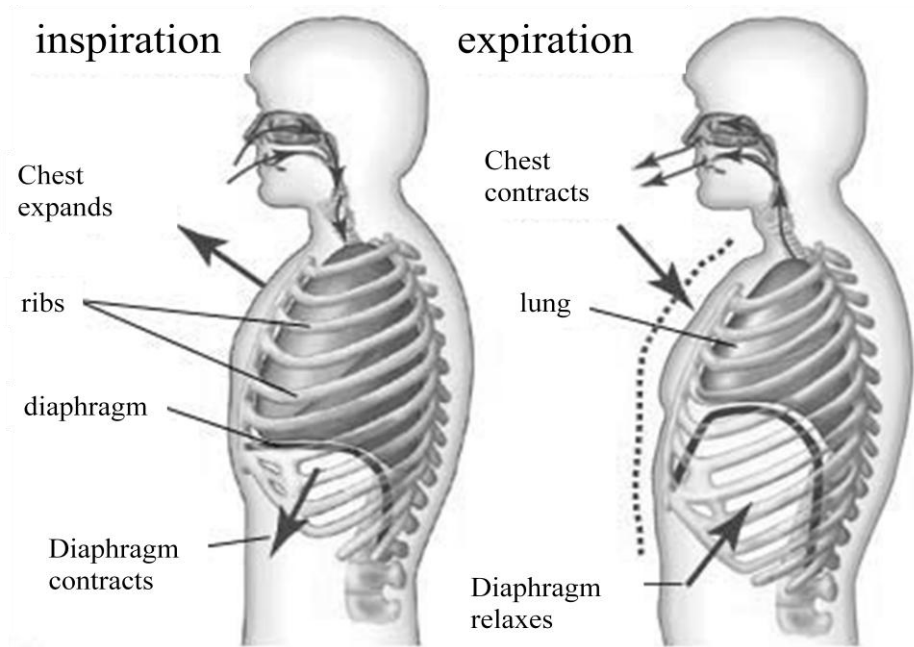


Fig.2. 3 Illustration of expiration and inspiration mechanisms in chest respiration

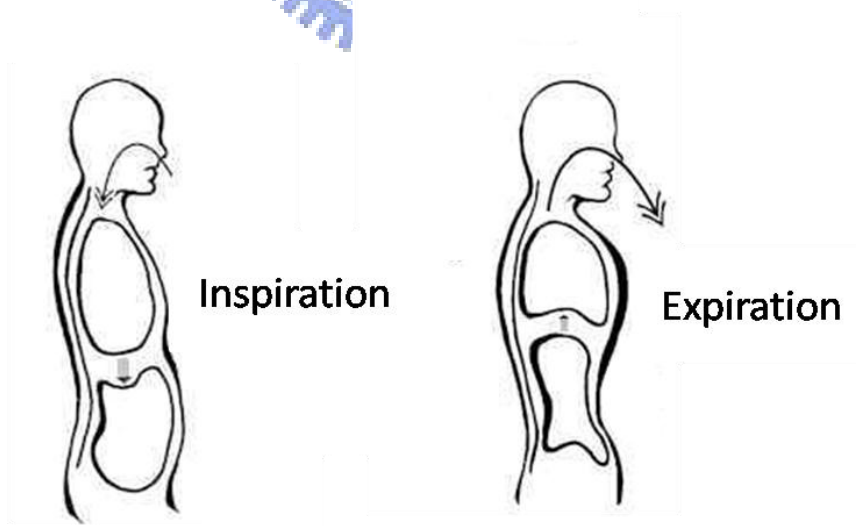


Fig.2. 4 Illustration of expiration and inspiration mechanisms in abdominal breathing

2.2 Evaluation of Respiratory Sinus Arrhythmia

(RSA)

2.2.1 Introduction to RSA

The theme of cardiorespiratory interactions has drawn the attention of researchers since more than 60 years ago. Among a number of quantitative factors proposed, respiratory sinus arrhythmia (RSA) has been widely used as an index to signify the phenomenon of heart rate variation in accordance with respiration activity. In recent years, this theory was further expanded to encompass a wide range of hypotheses regarding physical, psychophysiological and even social functioning in humans[15]. The heart-beating rhythm is primarily maneuvered by the vagus nerve that hinders heart rate and the contracting power as follows[16]:

inspiration → inhibition of vagus-nerve activity → increase of heart rate;

expiration → acceleration of vagus-nerve activity → decrease of heart rate.

As a consequence, the R-R interval of ECG is shortened during inspiration and prolonged during expiration. Fig.2.5 illustrates the RSA phenomenon of the heart-rate fluctuations associated with breathing. Apparently, heart rate accelerates during inspiration and decelerates during expiration.

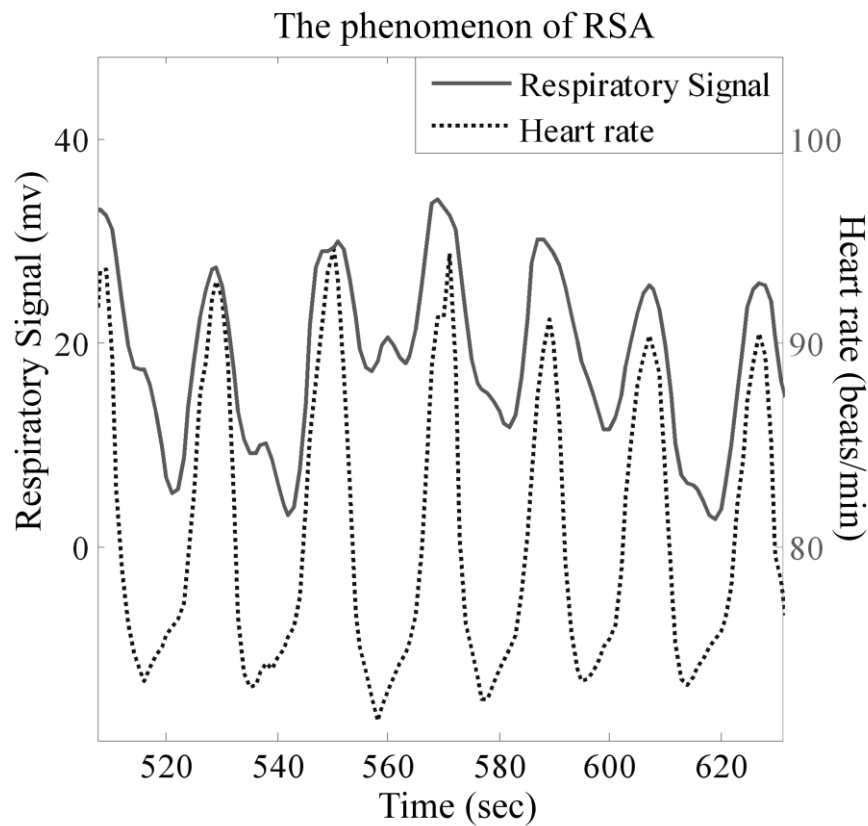


Fig.2. 5 RSA phenomenon illustrated by the increase (decrease) of heart rate during inspiration (expiration).

Since RSA has been widely used in psychophysiological research, different methods for quantifying RSA's have been proposed[17]. Distinctions among these methods are mainly the assumption regarding the operational definition of RSA and the dependence of RSA on respiration. For example, according to the above definition of RSA (that is, increased/decreased heart rate during inspiration/expiration), RSA can only occur in the presence of breathing. In fact, before the understanding of the neuro-anatomical structures and neuro-physiological mechanisms involved in regulating RSA, RSA was an observed phenomenon described by the measurement of heart rate and respiration.

RSA can be quantified by spectral analysis, time-domain peak-valley analysis, or application of band-pass filtering. RSA estimated in the time-domain is based on the analysis of the amplitude of heart rate fluctuations regulated by the breathing cycle. For example, the peak-valley method evaluates the difference between the fastest heart rate during inspiration and the slowest heart rate during expiration[18][19]. As a consequence, unit of measurement differs according to different physical meaning. In time-domain analysis, RSA is typically estimated in the scale of millisecond (ms). The inspiratory–expiratory difference in RRI (R-to-R interval of ECG) has been evaluated by this scheme[20].

.2.2 Evaluation of RSA

In this study, we quantify the RSA behavior by using the formula proposed in[21]. Firstly, an appropriate window size N_c is determined in the scale of number of breaths. For example, $N_c = 5$ indicates a window size of 5 breaths. The RRI (R-to-R interval) sequence is reconstructed from the ECG signal. In the i^{th} RRI epoch of N_c -breath duration, we first compute the average of positive-peak values $\overline{P_i^+}$ and the average of negative-peak values $\overline{P_i^-}$ within the RRI epoch. Then, the RSA rate R_{RSA} is estimated by the normalized difference in the following formula[17][21]:

$$R_{RSA}(i) = \frac{\overline{P_i^+} - \overline{P_i^-}}{RR_i} = \frac{\frac{1}{N_{P^+}} \sum_{l=1}^{N_{P^+}} P_i^+(l) - \frac{1}{N_{P^-}} \sum_{l=1}^{N_{P^-}} P_i^-(l)}{\frac{1}{N_{RR}} \sum_{l=1}^{N_{RR}} RR_i(l)}, \quad (2.1)$$

where

$P_i^+(l)$: the l^{th} positive-peak value in the i^{th} RRI epoch,

$P_i^-(l)$: the l^{th} negative-peak value in the i^{th} RRI epoch,

\overline{RR}_i : the average value (DC) of the i^{th} RRI epoch,

$N_{P+}(N_{P-})$: number of positive (negative) peaks in the i^{th} RRI epoch,

N_{RR} : number of RRI sample data in the i^{th} RRI epoch.

$$\overline{RR}_n \quad \forall n = 1, 2, 3, 4$$

2.3 Correlation coefficient

Correlation coefficient can be used to measure the degree of correlation or dependence between two observed variables. Such analysis thus allows us to explore possible causal relationships or underlying mechanism. In this study, we applied Pearson product-moment correlation coefficient to the evaluation of dependence between RSA rate and respiratory rate. This approach has been widely used and well justified to be feasible to be feasible for quantifying linear relationship. The formula to calculate correlation coefficient is

$$\gamma = \frac{S_{XY}}{S_X S_Y} \quad (2.2)$$

Where

$$S_{XY} = \sum_{n=1}^N \frac{1}{N-1} (\mathbf{X}[n] - \bar{X})(\mathbf{Y}[n] - \bar{Y}) \quad (2.3.1)$$

$$S_X^2 = \sum_{n=1}^N \frac{1}{N-1} (\mathbf{X}[n] - \bar{X}) \quad (2.3.2)$$

$$S_Y^2 = \sum_{n=1}^N \frac{1}{N-1} (\mathbf{Y}[n] - \bar{Y}) \quad (2.3.3)$$

Note that S_x and S_y denote respectively the standard deviation of the series of N measurements of \mathbf{X} : $\{x_i, 1 \leq i \leq N\}$ (respiratory rate) and \mathbf{Y} : $\{y_i, 1 \leq i \leq N\}$ (RSA rate), and S_{XY} is the covariance of X and Y .

\bar{X} : mean of respiratory rate ,

\bar{Y} : mean of RSA rate,



Chapter 3

Experiment and Signal Analysis

In this chapter, the experimental environment and procedure are first introduced. Then we introduce the methods for quantifying RSA for analyzing cardio-respiratory behaviors. How to best select the strategies and implementing parameters in these methods are presented.

3.1 Experimental Setup and Procedure

This study involved two groups of subjects, the experimental group including subjects with Zen-meditation experience and the control group including subjects without any meditation experience. Background of subjects in each group is listed in Table.3.1

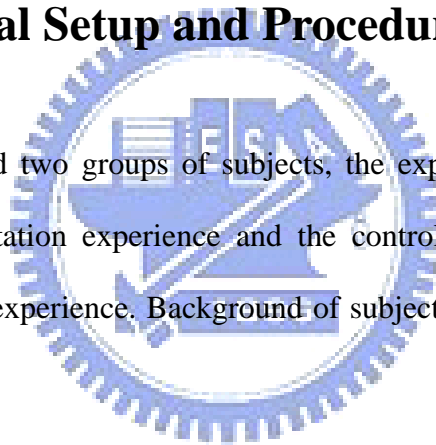


Table.3. 1 Subjects of experimental and control groups

	Experimental group	Control group
Number of subjects	6	6
Sex (male : female)	0:6	5 : 1
Age (years)	27.6 ± 2.3	26 ± 1.1
Meditation experience (years)	6 ± 1.9	

3.1.1 Control Group

In the experiment, we collected 30-min ECG and respiration signals for each subject. In the control group, each recording involved four sessions in which the subject was asked to breathe at different rates. In the first 5-minute session, the subject breathed naturally at their normal breathing rate. In the following two sessions of 10-minute duration each, the subject was asked to follow an auditory-cue guidance to breathe at the rate of respectively 10 and 6 breaths per minute. Finally, the subject breathed again at the normal rate in the fourth 5-minute session. Fig.3.1 illustrates the experimental procedure.

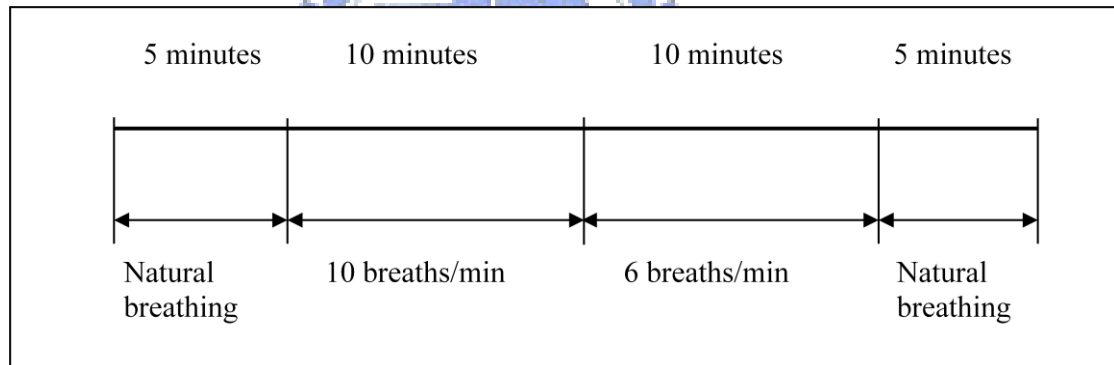


Fig.3. 1 Experimental procedure for the control group. Four sessions include (1) baseline measurement (5 minutes), (2) breath control at 10 breaths/min (10 minutes), (3) breath control at 6 breaths/min (10 minutes), and (4) post-test natural breathing (5 minutes).

3.1.2 Experimental Group

ECG and respiration signals of experimental subjects (Chan-meditation

practitioners) were collected while they practiced Chan meditation in the meditation course held in a formal meditation center. Subjects were not required to follow any protocol, instead, they only took part in their routine practice in the 90-minute class as usual. Appendix B briefly describes the procedure of the practice.

After the Chan-meditation class, subjects were interviewed immediately. The oral report of their meditation scenario was recorded.

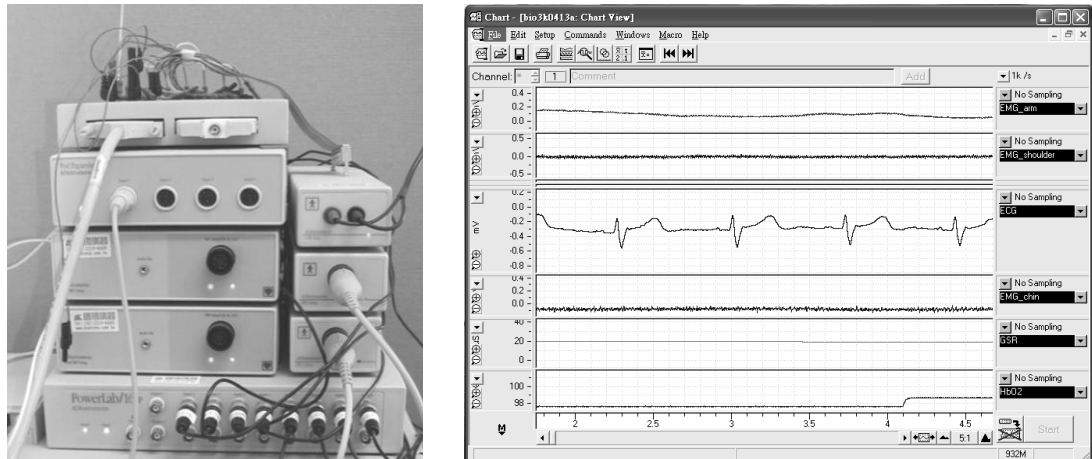
3.1.3 Signal Acquisition

Fig.3.2 demonstrates the recording system for collecting the physiological signals employed in the control group. The signals recorded from a subject are amplified, pre-filtered and digitized by g.BSamp biosignal amplifier manufactured by Cortech Solutions. The digital signals are transmitted to a desktop through USB interface and then recorded with the built-in data-acquisition software (Chart4). The ECG and respiratory signals were recorded by the system simultaneously and digitized with a sampling frequency of 1,000 Hz.

The ECG and respiration signals were recorded simultaneously at 1000 Hz sampling rate using PowerLab/16SP recording system (ADInstruments, Sydney, Australia; see Fig. 3.2). Furthermore, the ECG signal was pre-filtered by a 0.3-200 Hz bandpass filter, and the respiratory signal was pre-filtered by a lowpass filter with cutoff frequency of 5 Hz. A 60-Hz notch filter was applied to remove artifacts from power line or the surroundings.

For experimental group, the electrocardiogram (ECG) and respiration signals were recorded simultaneously at 512Hz and 128Hz using NuXus-4 recording system (TMS

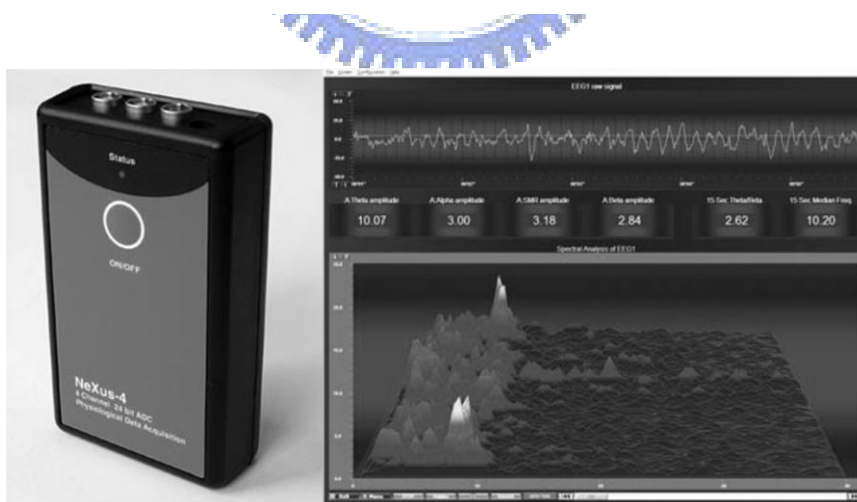
International BV, Oldenzaal, The Netherlands; see Fig.3.3). The respiratory signals was recorded using a piezo-electric transducer (NX-RSP1A, TMS International BV, Oldenzaal, the Netherlands) wrapped around the belly passing the navel.



(a)

(b)

Fig.3. 2 Physiological signal recording system for control group: (a) Bio-amplifiers, and (b) digitization and on-line monitoring system.



(a)

(b)

Fig.3. 3 Physiological signal recording system for experimental group: (a) Bluetooth Bio-amplifiers, and (b) digitization and on-line monitoring system.

3.1.4 Measurement of ECG signal

The recording electrodes (Medi-Trace 200 Foam Electrode) are manufactured by Kendall-LTP, as shown in Fig. 3.4 (a). In this study, the ECG recording applied the bipolar limb-lead I electrode placement in control group and applied the bipolar limb-lead II electrode placement in experimental group. By convention, limb-lead I has the positive electrode on the left arm, and the negative electrode on the right arm, with an electrode on the right leg serving as a reference electrode. Such kind of bipolar configuration accordingly measures the potential difference between two arms. For convenience of applying electrodes to voluntary subjects, we adjusted the placement by attaching the positive/negative electrode to the left/right inner wrist, with the reference electrode placed on the right ankle (Fig 3.4).

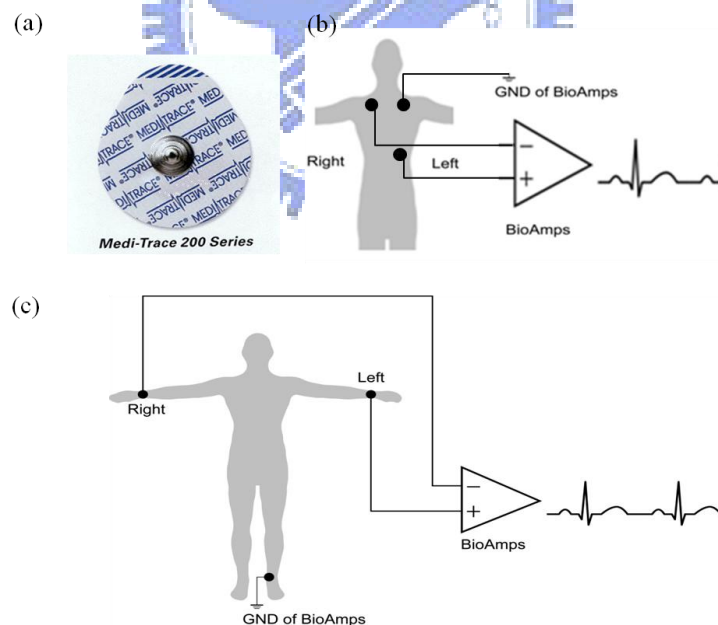


Fig.3.4 (a) ECG electrode, (b) Bipolar limb-lead II electrode placement(experimental group) and (c) Bipolar limb-lead I electrode placement(control group).

3.1.5 Measurement of respiratory signal

The behavior of respiration accompanying the chest/abdominal movement is recorded by the piezo-electric transducer (Model 1132 Pneumotrace II (R)) made by UFI, as shown in Fig. 3.5. The electrical conductivity increases linearly with the chest/abdominal circumference associated with respiration, and the sine-wave like signal can be recorded. Fig 3.6 demonstrates the waveform pattern during inspiration and expiration. The pattern exhibits a positive slope at inspiration, and a negative slope at expiration, reflecting the expanding and contracting movement of the chest/abdomen.



Fig.3. 5 Piezo-electric respiratory transducer.

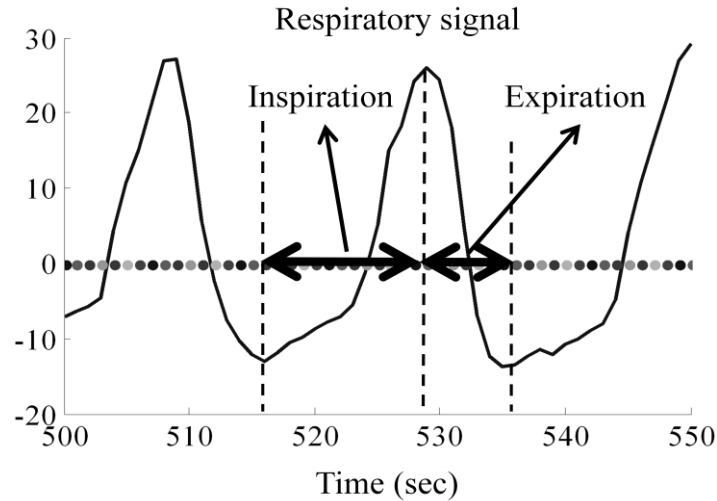


Fig.3. 6 Respiratory signal

3.2 Strategy for RSA Quantification

This section introduces the strategy for investigating the cardio-respiratory interactions via RSA analysis. The strategy mainly involves three steps, 1) pre-processing of ECG and respiratory signals, 2) quantification of RSA phenomenon, and 3) interpretation of results.

In the first step, peak-detection algorithm and re-sampling scheme were applied to ECG and respiratory signals. We then obtained the reconstructed RRI (R-to-R interval) sequence and the time-varying respiration rate. In the second step, we developed appropriate methods and algorithms to quantify RSA phenomenon. Finally, we designed the scheme for interpreting the results based on different control factors.

Step 1 Pre-processing

ECG and respiratory signals were recorded using PowerLAB biosignals recording system (AD Instrument, Australia). The ECG was pre-filtered by a 0.3-200 Hz bandpass filter and digitized by a sampling rate of 1,000 Hz. The RRI sequence was reconstructed by (i) detecting the time of occurrence of each R peak, and (ii) linearly interpolating the RRI samples to make a digital signal equivalent to 200Hz sampling rate. Heart rates, average R-R interval and the standard deviation of the R-R intervals were computed from the reconstructed RRI sequence. Then the algorithms described in Appendix A were applied to the detection of R peaks of ECG and peaks of respiratory signal.

Step 2 RSA quantification

Fig.3.7 illustrates the signal flow graph for estimating RSA rate. Considering the window size of five breaths ($N_c=5$), the parameters determined from the empirical data are marked in Fig 3.8. Fig 3.9 displays the result of RSA analysis for a subject in the breathing control experiment.

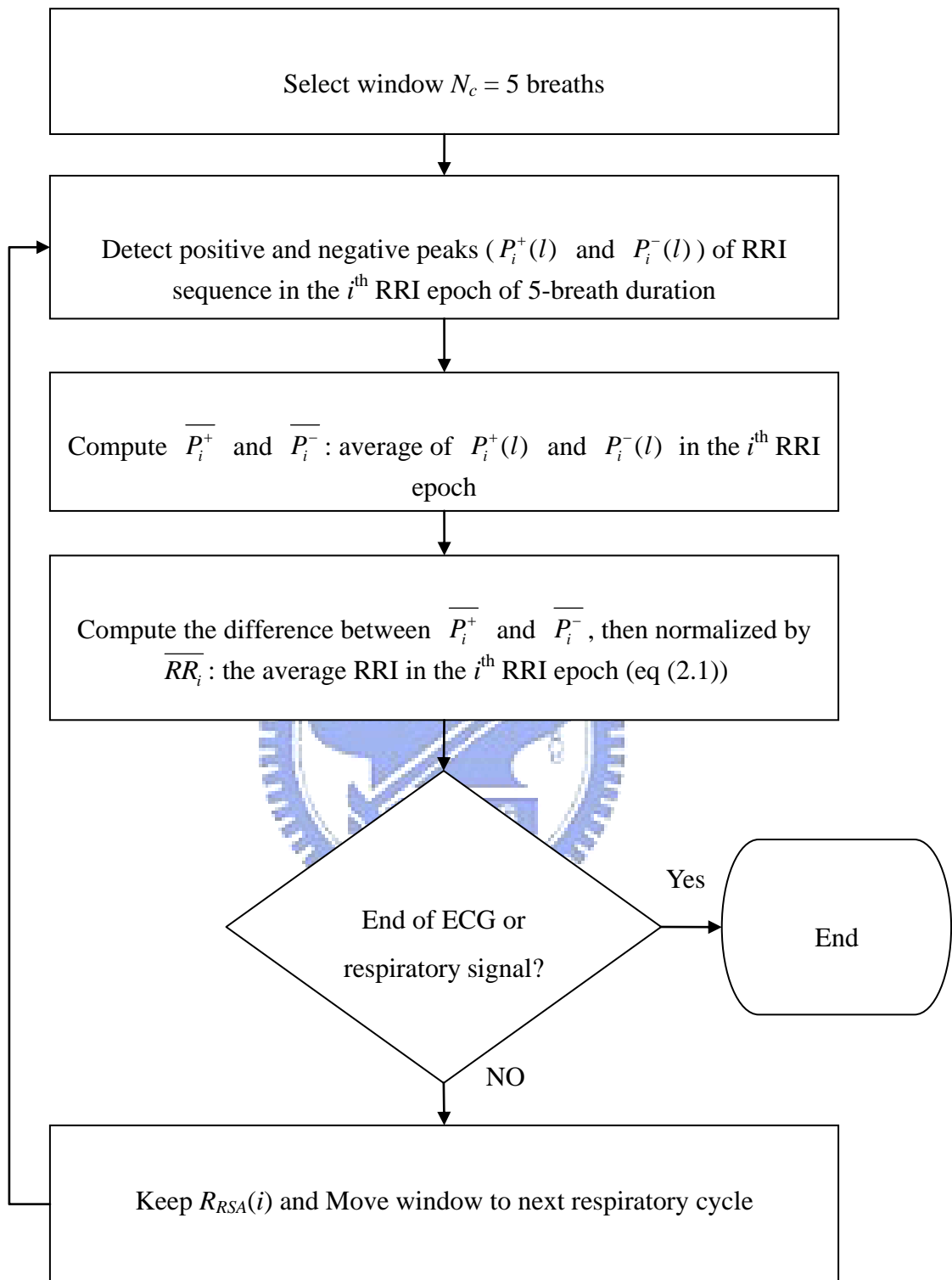


Fig.3. 7 Signal flow graph for RSA quantification.

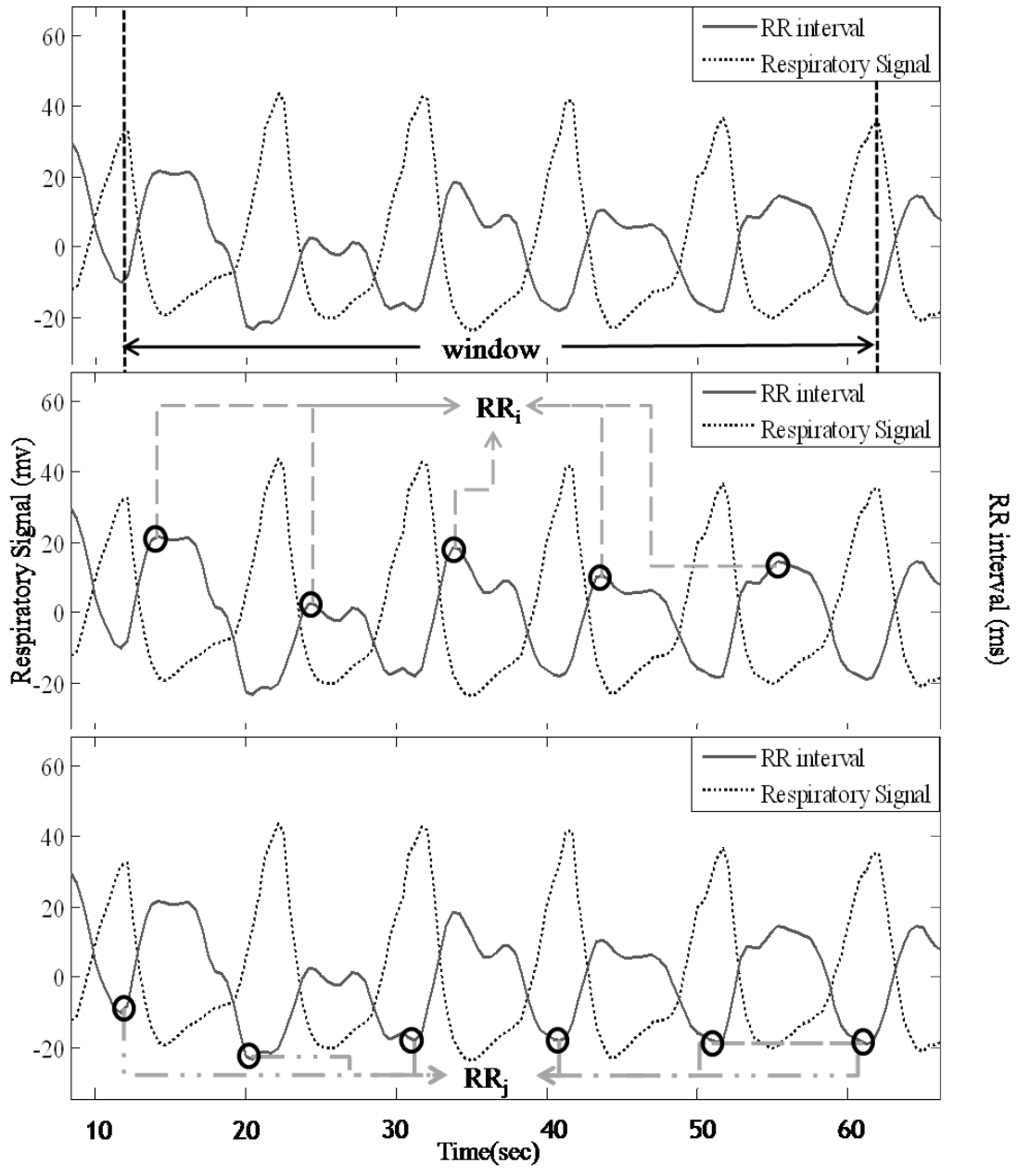


Fig.3. 8 (a) This example uses five respiratory cycles as a window to calculate RSA rate. (b) Based on a window size of five respiratory cycles, we may find five local maximum points of RR_i . (c) Based on a window size of five respiratory cycles, we may find five local minimum points of RR_j .

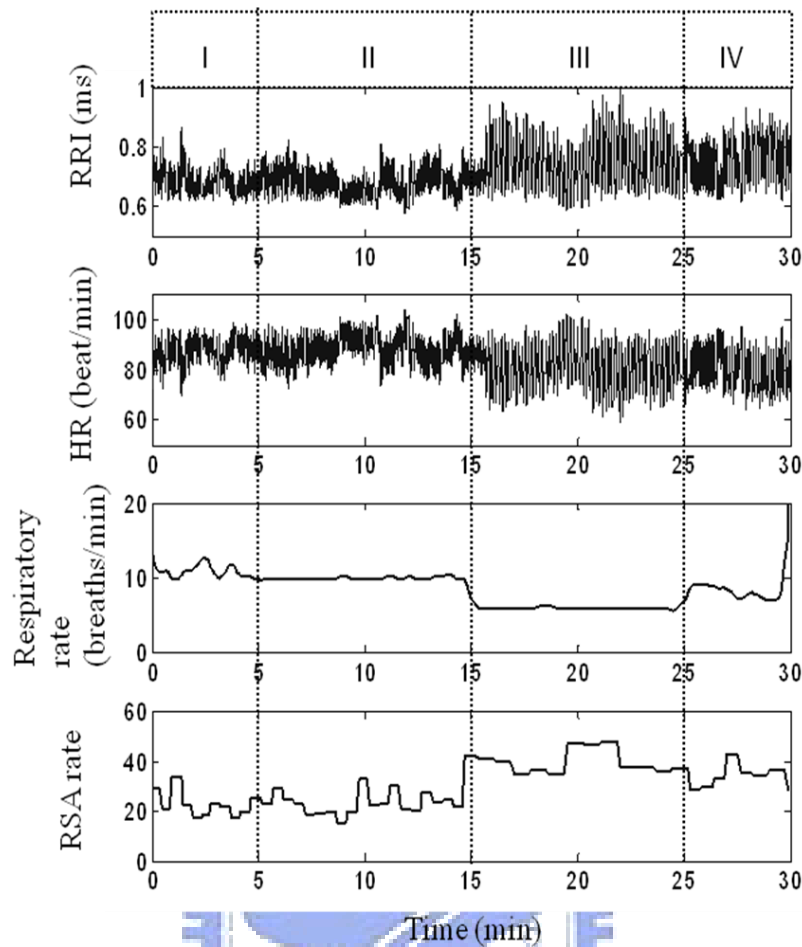


Fig.3. 9 Sequences of RRI, heart rate, RSA rate and respiratory rate, from the top. In (I) and (IV) sessions, the subject breathed normally at their natural breathing rate. In (II) and (III) sessions, the subject followed an auditory-cue guidance to breathe at the rate of respectively 10 and 6 breaths per minute.

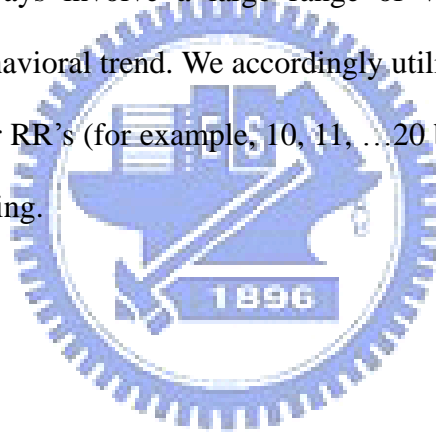
3.3 Statistical Evaluation

The complexity of human life system often results in difficulty of identifying the actual causality (the relationship between the cause and the effect) from multifactor (multivariate) control mechanism. To deal with this issue, we analyzed the relationship between respiratory rate (RR) and RSA rate in three heart-rate (HR)

ranges.

As illustrated in Fig 3.10, We first sort the HR samples in ascending order and then divide them into three sections (slow, medium, and fast HR), each containing equal number of HR samples. The samples of RR (respiratory rate) and R_{RSA} (RSA rate) are then grouped into 3 clusters corresponding to slow, medium and fast HR. Correlation coefficient is computed by applying equation (2.2) to each cluster to observe if there exists either positive or negative correlation between respiratory rate and RSA rate.

Empirical data always involve a large range of variation that obscures the identification of core behavioral trend. We accordingly utilize the mean values of R_{RSA} computed at each integer RR's (for example, 10, 11, ...20 breaths/min) to conduct the linear-regression line fitting.



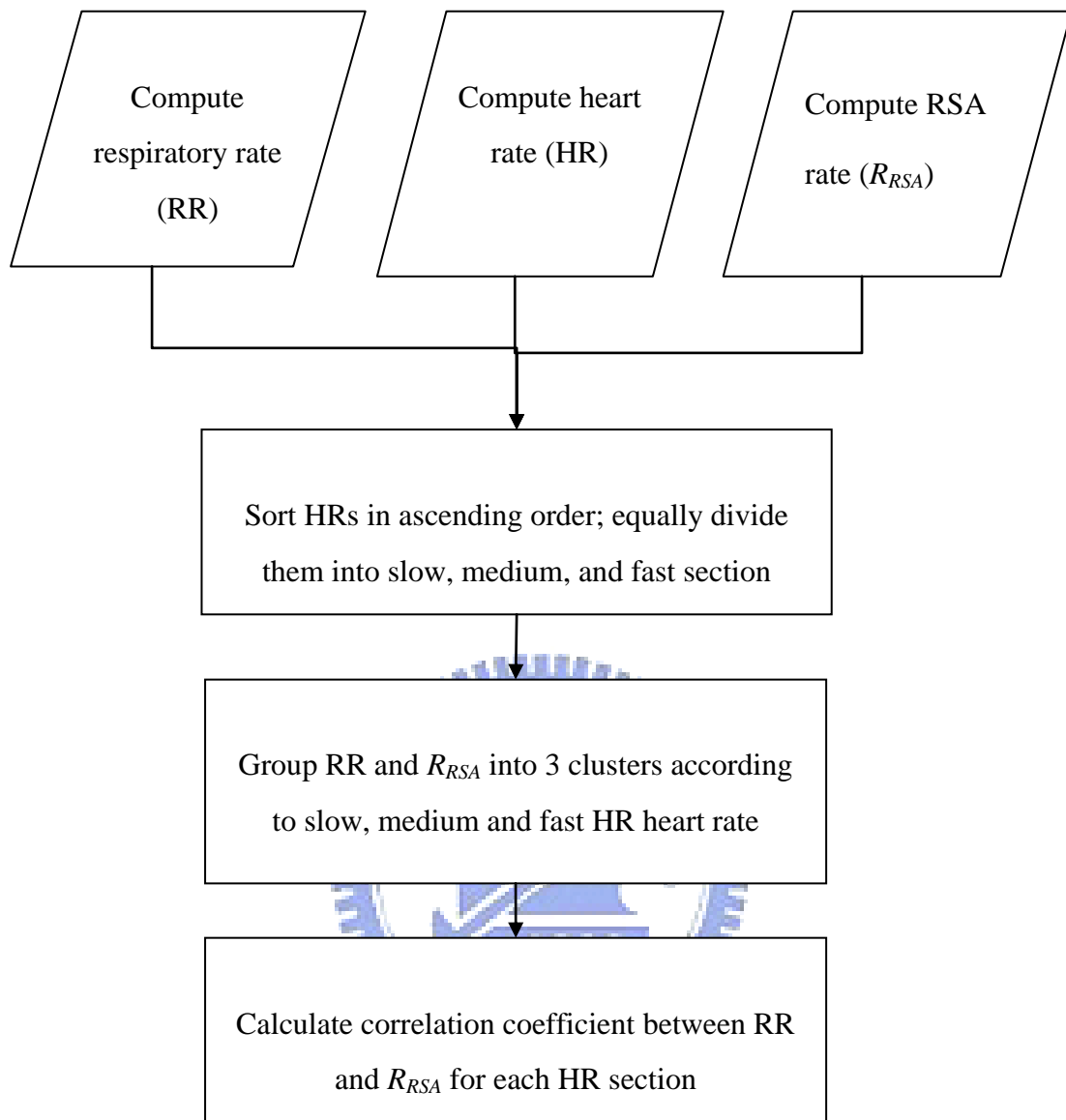


Fig.3. 10 Signal flow graph of evaluating correlation coefficients between respiratory rate and RSA rate in the slow, medium, and fast HR range.

Chapter 4

Experimental Results And Analysis

This chapter presents the results of RSA analysis and statistical analysis between respiratory rate and RSA rate for both groups. Section 4.1 reports the results of RSA rate analysis for both groups. The correlations between RSA rate and respiratory rate are discussed in Section 4.2.

4.1 Results of RSA analysis

This study was based on the hypothesis that parasympathetic nervous system would be enhanced when slowing down the respiratory rate. Statistical analysis was conducted to justify the significance of effect of control factors (in this study, the respiratory rate). For the control group, we employed the paired-sample t-test to the RSA rate during the second (10 breaths/min) and third session (6 breaths/min). As regards the experimental group, we will only present the time-dependent RSA rates for each subject since no control-factor intervention was employed. In that case, meditation scenario and quality cannot be secured in the entire recording.

Time-dependent RSA rates for the control and experimental subjects are shown, respectively, in Figs 4.1 and 4.2. RSA rate of all six control subjects appears to have little change when proceeding from Session I (natural breathing) to Session II (breathing control at 10 breaths/min), which shows a considerable increase in Session III (breathing control at 6 breaths/min).

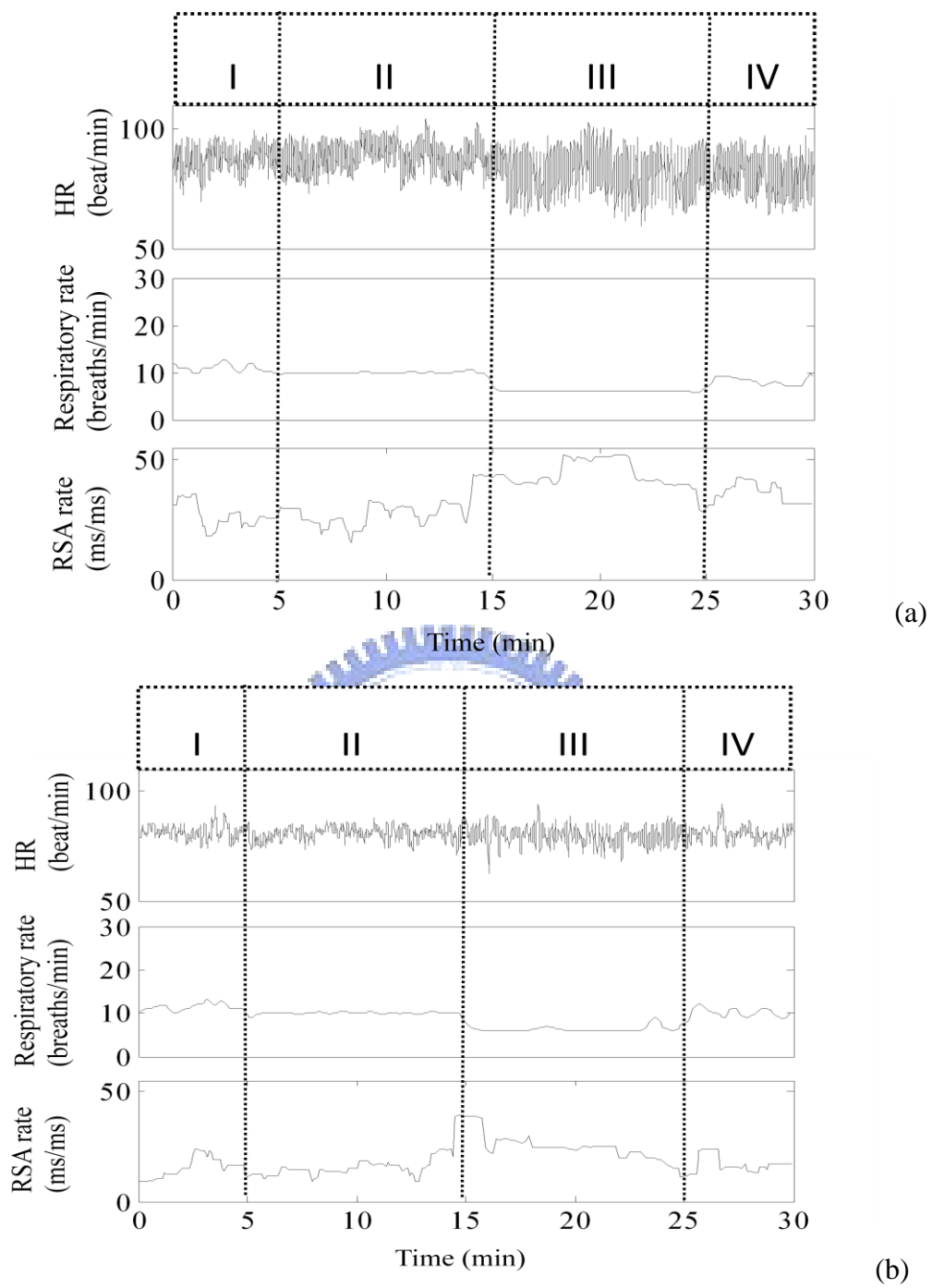
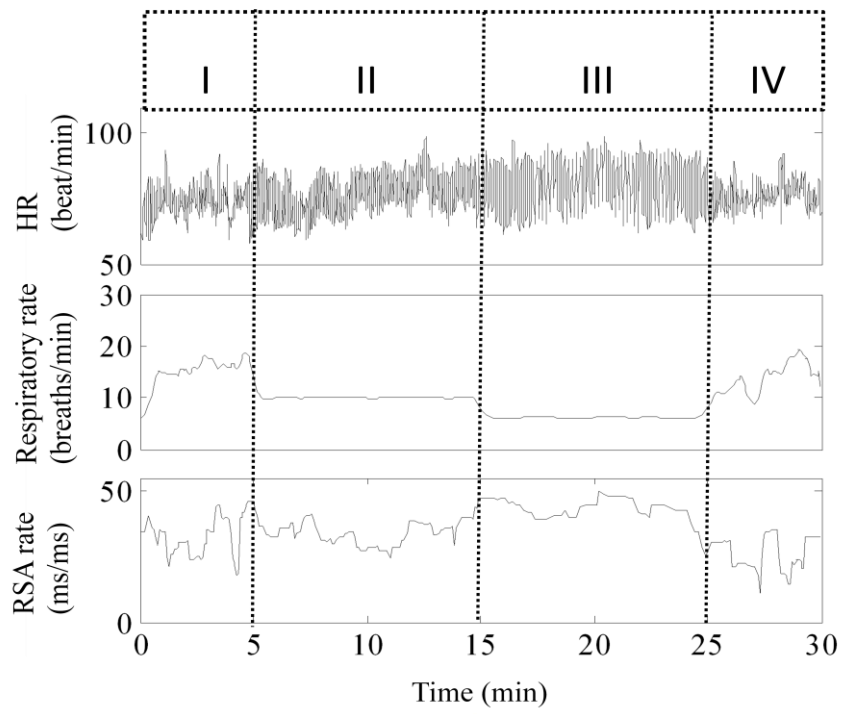
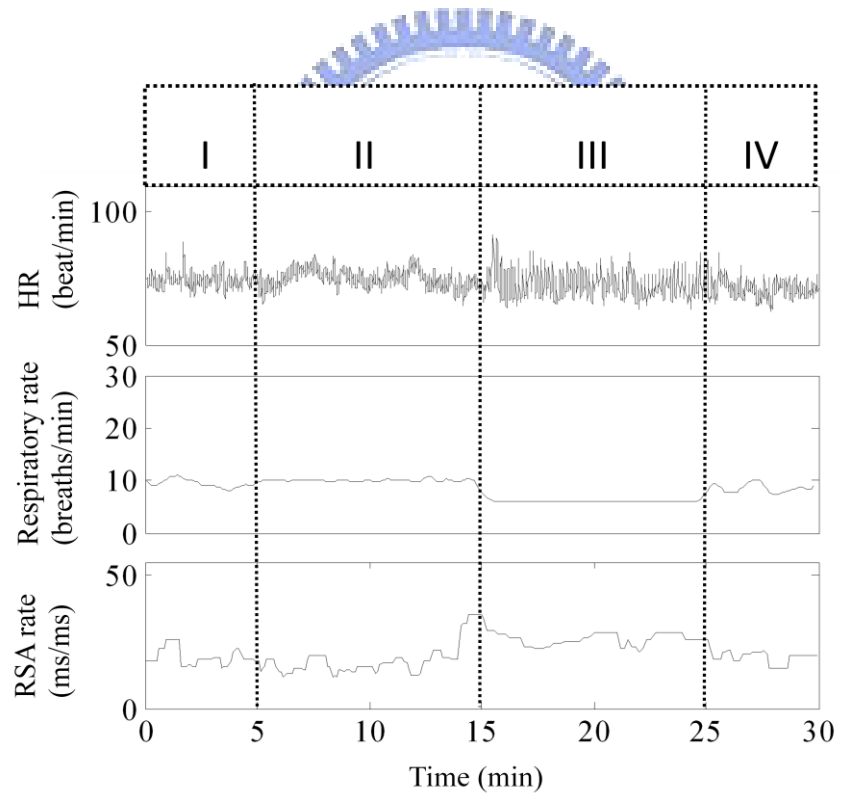


Fig.4. 1. Time-dependent RSA rates for control subject 1 (a)-(f) show the results for subject 1-6 respectively.

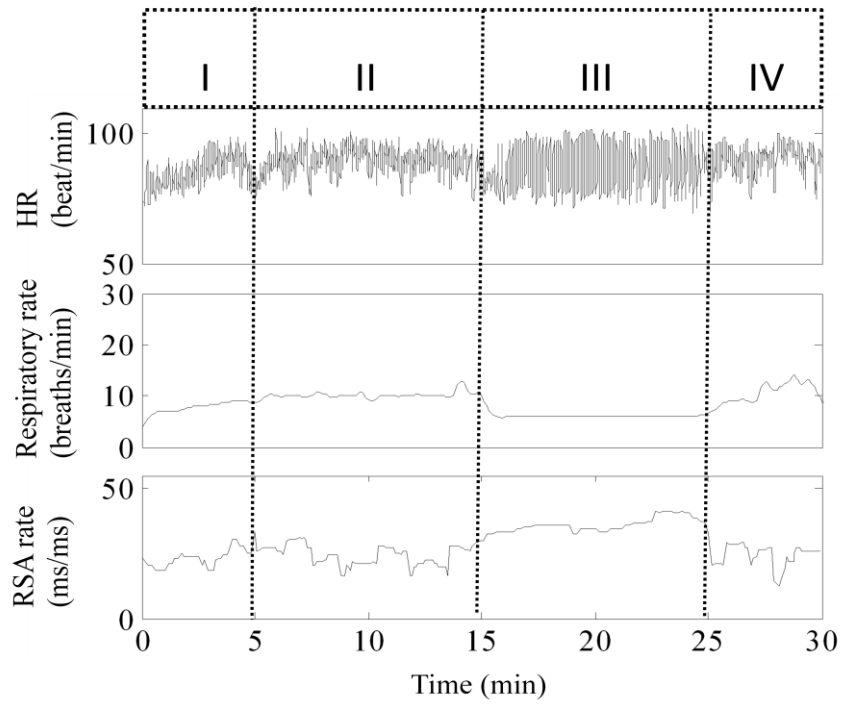


(c)

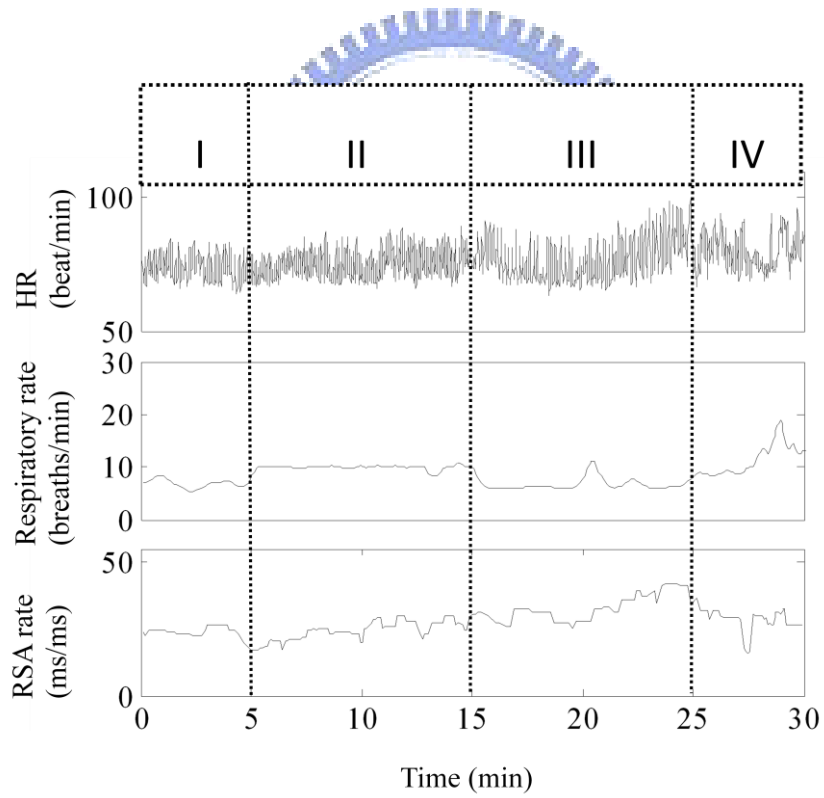


(d)

Fig.4. 1. Continue.



(e)



(f)

Fig.4. 1. Continue.

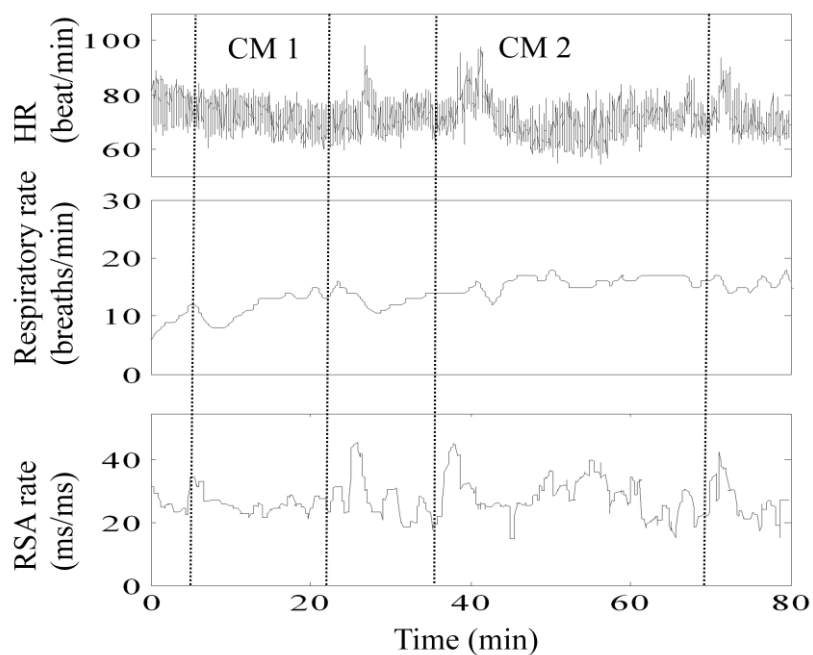


Fig.4. 1.(a) Time-dependent RSA rates for experimental subject 1 (a)-(f) show the results for subject 1-6 respectively.

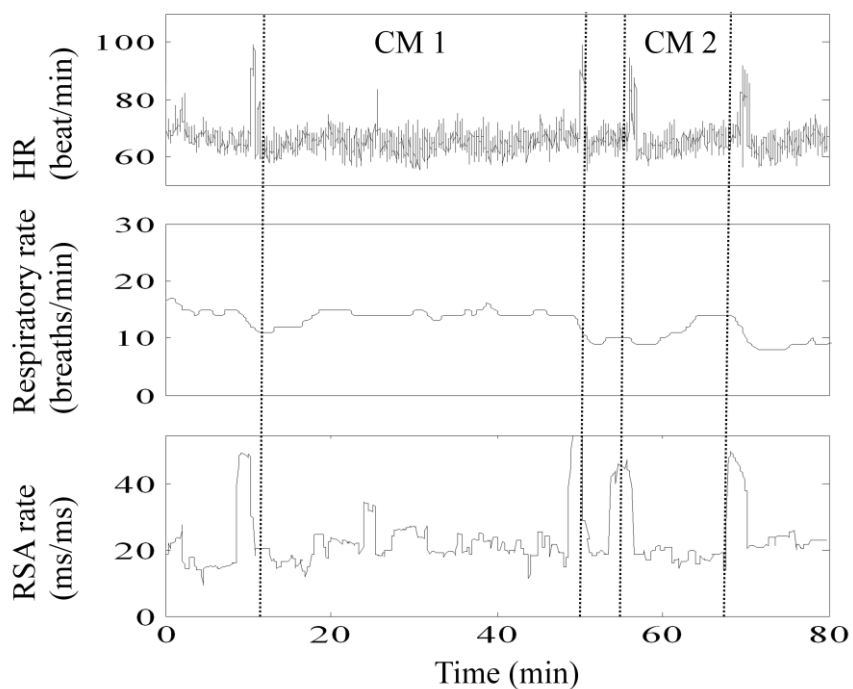


Fig.4. 2.(b) Continue

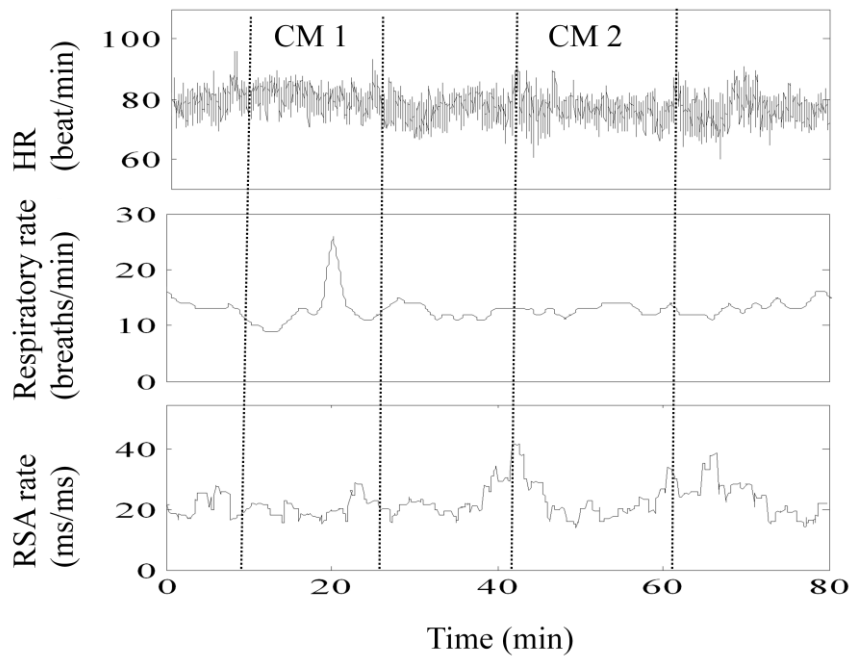


Fig.4. 2.(c) Continue

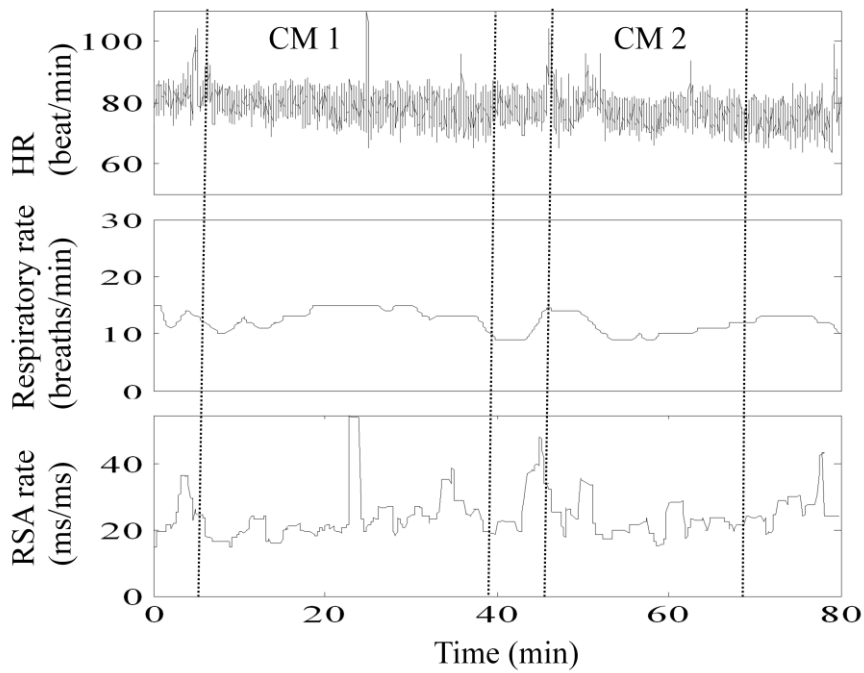


Fig.4. 2.(d) Continue

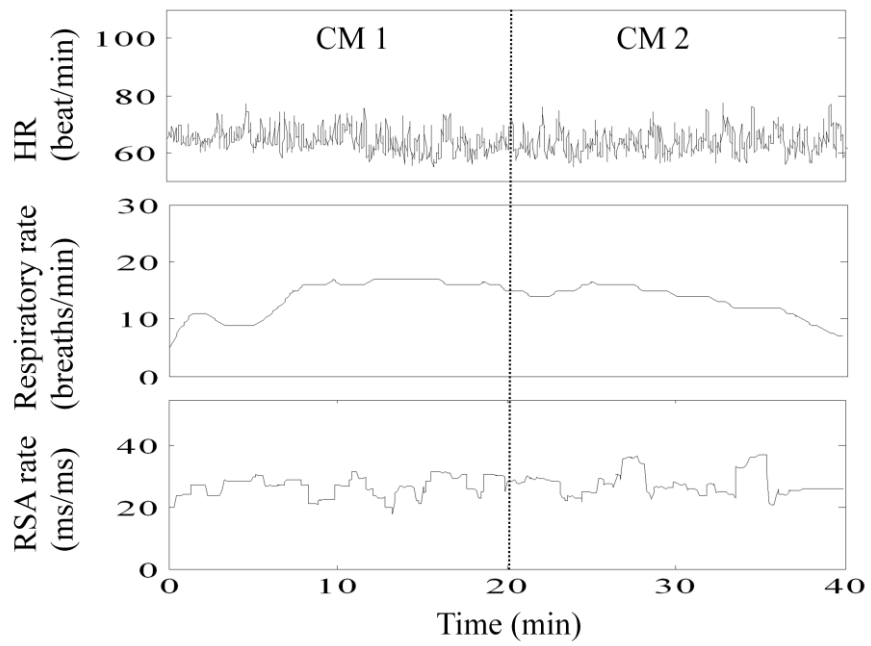


Fig.4. 2.(e) Continue

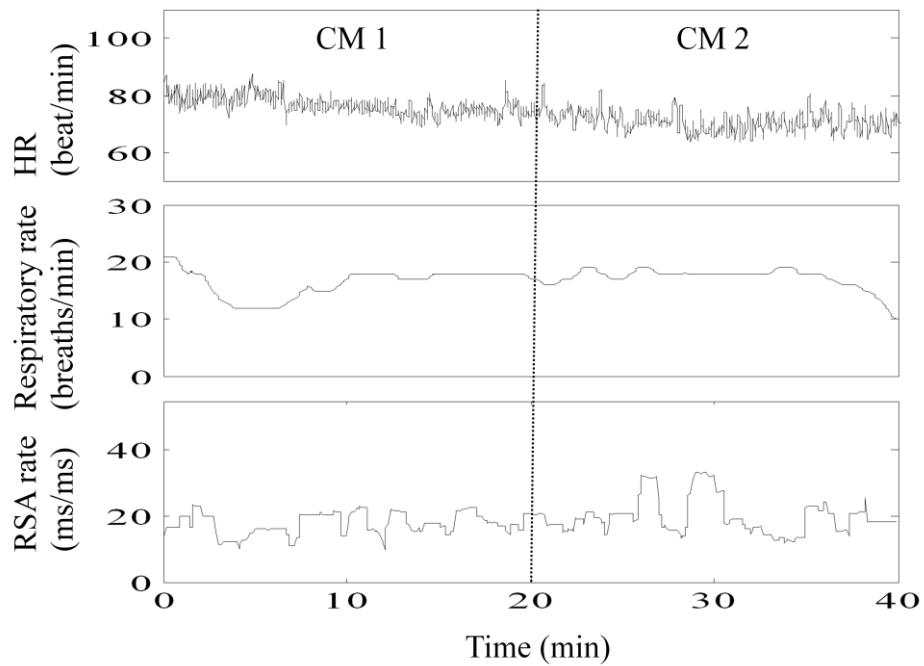


Fig.4. 2.(f) Continue

Fig. 4.3 displays the averages and standard deviations of RSA values in Session II and Session III. According to the implementation strategy described in Chapter 3, there will be approximately 100 R_{RSA} samples in Section II and 60 R_{RSA} samples in Section III, with window size of 5 breathing cycles and moving step of 1 breathing cycle. From (a) to (f), results of six control subjects all demonstrate the increase of RSA from Session II to III. By employing SPSS to the RSA rates, we may conclude the statistically significant difference between Sessions II and III ($p < 0.05$). Table.4.1 summarizes the results with p values.

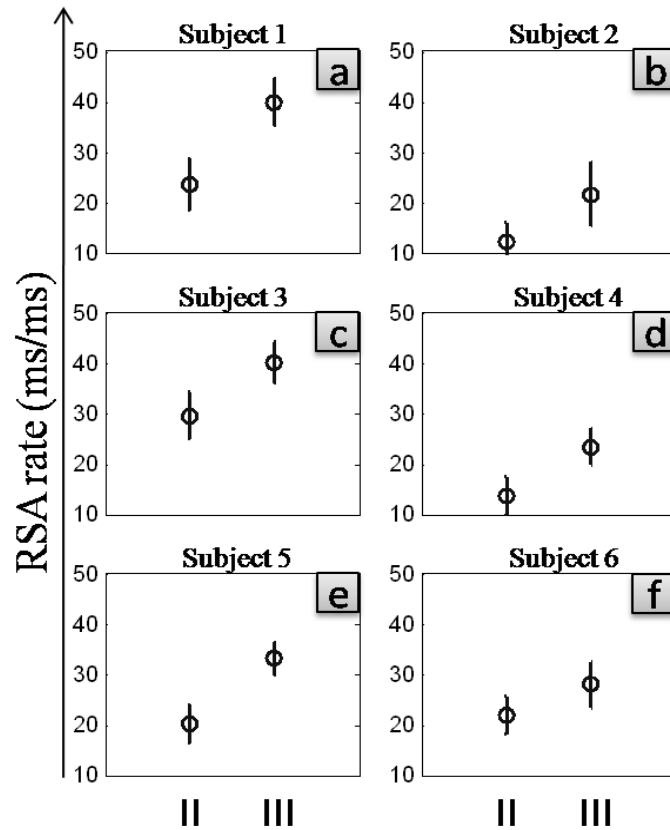


Fig.4. 2 Average and standard deviation of RSA values in Session II and Session III.

From (a) to (f), results of six control subjects all demonstrate the increase from Session II to III.

Table.4. 1 Average and standard deviation of RSA values for 6 control subjects in Sessions II and III. Statistical significance of the difference between these two sessions is apparent ($p<0.05$).

	10 breathing/min		6 breathing/min		<i>P value</i>
	mean	std	mean	std	
subject1	14.977	3.990	19.698	7.354	$p<0.05$
subject2	6.238	2.676	9.156	6.707	$p<0.05$
subject3	16.185	3.817	30.874	7.480	$p<0.05$
subject4	22.071	5.009	30.676	8.508	$p<0.05$
subject5	8.335	2.364	17.887	2.994	$p<0.05$
subject6	12.364	4.558	25.568	6.767	$p<0.05$

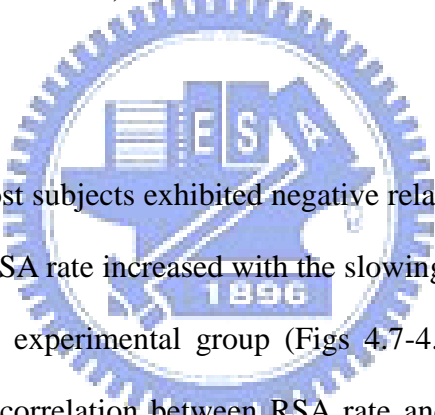
4.2 RSA rate and respiratory rate

According to Table.4.1, RSA rate increases when respiratory rate decreases from 10 breaths/min to 6 breaths/min. To extensively investigate the RSA dependency on respiratory rate, we sketched the RSA rate versus respiratory rate (RR) and analyzed the correlation coefficients based on equations (2.2) and (2.3.1)-(2.3.3). To exclude the bias of heart rate in multivariate controlling mechanisms, the entire data were sorted by heart rate (HR) and divided into three groups (fast, medium, and slow) of

HR containing equal number of samples.

4.2.1 Results for individual subject

The flow chart illustrated in Fig 3.10 was adopted to analyze the relation between RSA rate and respiratory rate for each individual subject. Figs 4.4-4.6 display the RSA rate versus respiratory rate respectively in the fast, medium and slow HR range for each control subject. Figs 4.7-4.9 display the RSA rate versus respiratory rate respectively in the fast, medium and slow HR range for each experimental subject during the first meditation session, while results for the second meditation session are plotted in Figs 4.10-4.12.



In control group, most subjects exhibited negative relation between RSA rate and respiratory rate, that is, RSA rate increased with the slowing down of respiration (Figs 4.4-4.6). Whereas in the experimental group (Figs 4.7-4.12), we begin to observe some dominant positive correlation between RSA rate and respiratory rate in some practitioners (particularly, subjects #4 and #5). Such interesting contradiction between two groups arouses our attention. Based on our understanding of the core practice of *heart-purification* Chan meditation, practitioners often experience some halo-light energy surrounding the Heart Chakra during meditation. Such phenomenon might be the factor that speeds up the heart beating. Since Chan meditation mostly harmonizes the operation of different organ systems in the body, RSA rates might be maintained at a stable level. It appears that normal healthy subjects (control group) may well induce the RSA rate by slowing down respiration with constant breathing rate for a considerable duration. On the other hand, there still leave some uncertainties

regarding the dependency of RSA rate on respiration for the Chan-meditation mechanism. These issues will be further investigated by appropriate experimental protocol in the future.

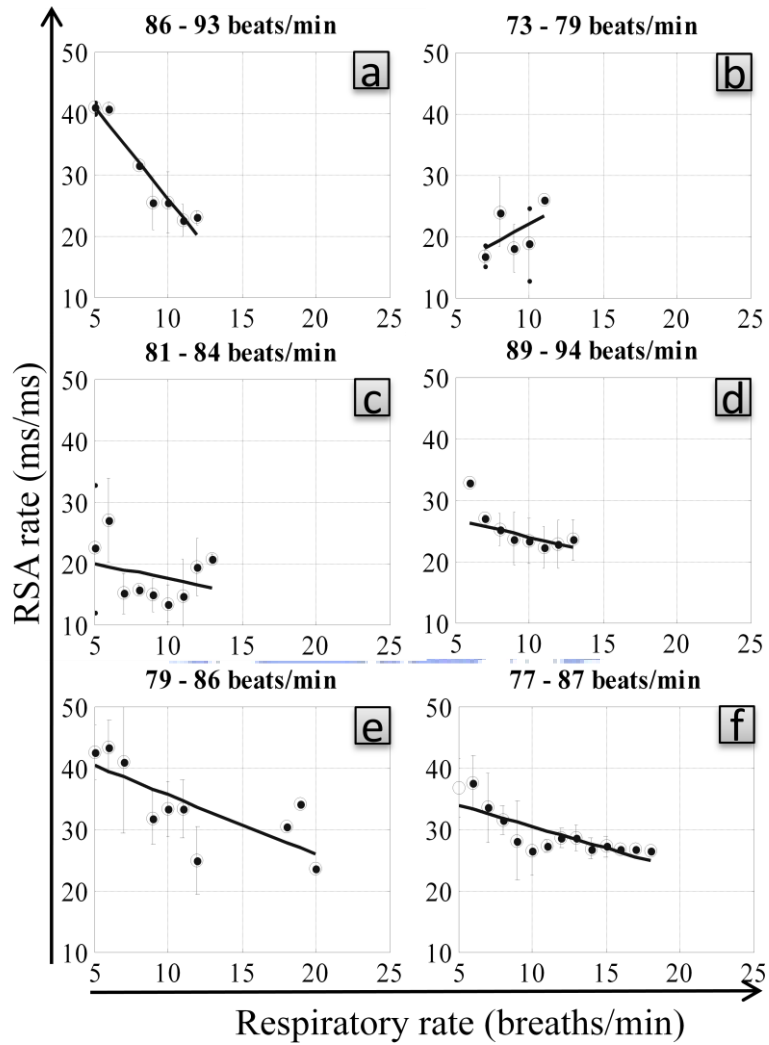


Fig.4. 3 RSA rate versus RR in the fast HR range for control subject 1-6 (from (a) to (f)).

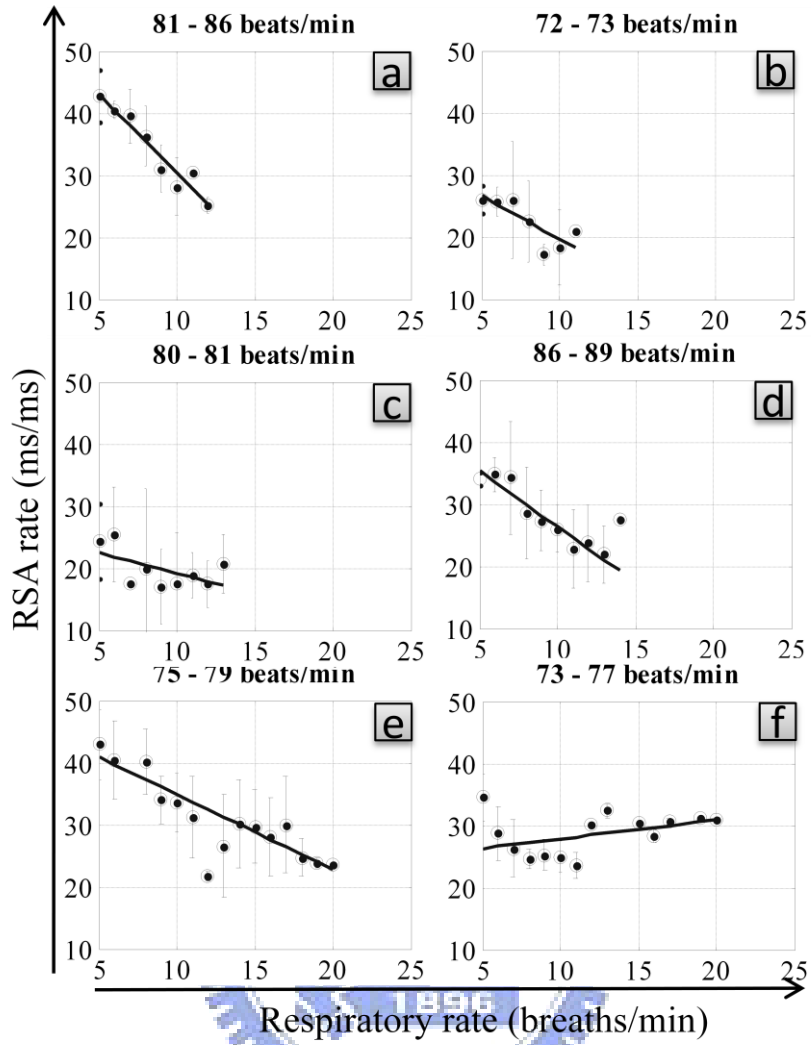


Fig.4. 4 RSA rate versus RR in the medium HR range for control subject 1-6 (from (a) to (f)).

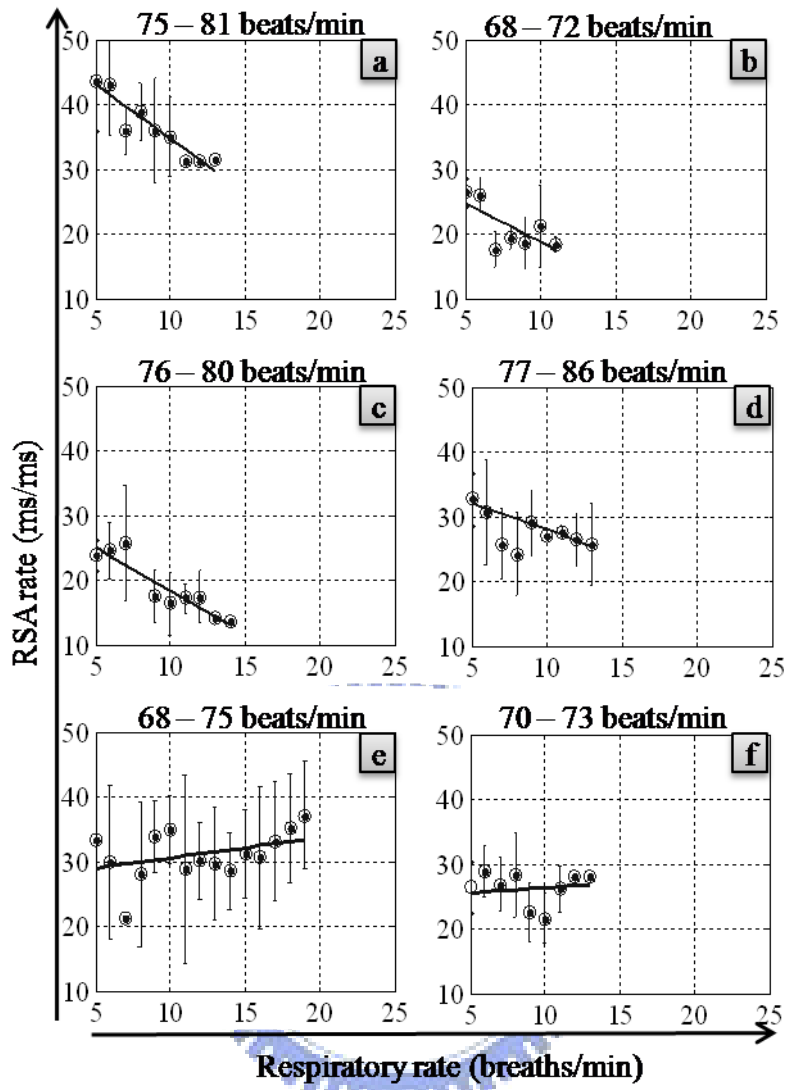


Fig.4. 5 RSA rate versus RR in the slow HR range for control subject 1-6 (from (a) to (f)).

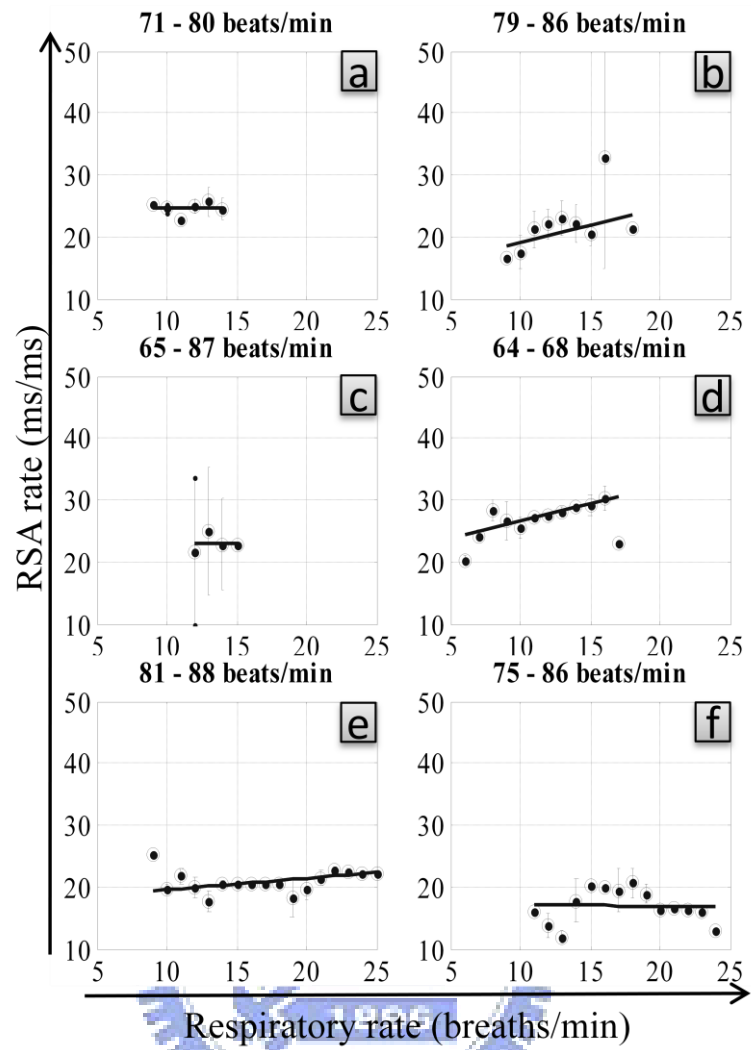


Fig.4. 6 RSA rate versus RR in the fast HR range for experimental subject 1-6 (from (a) to (f)) during the first meditation session.

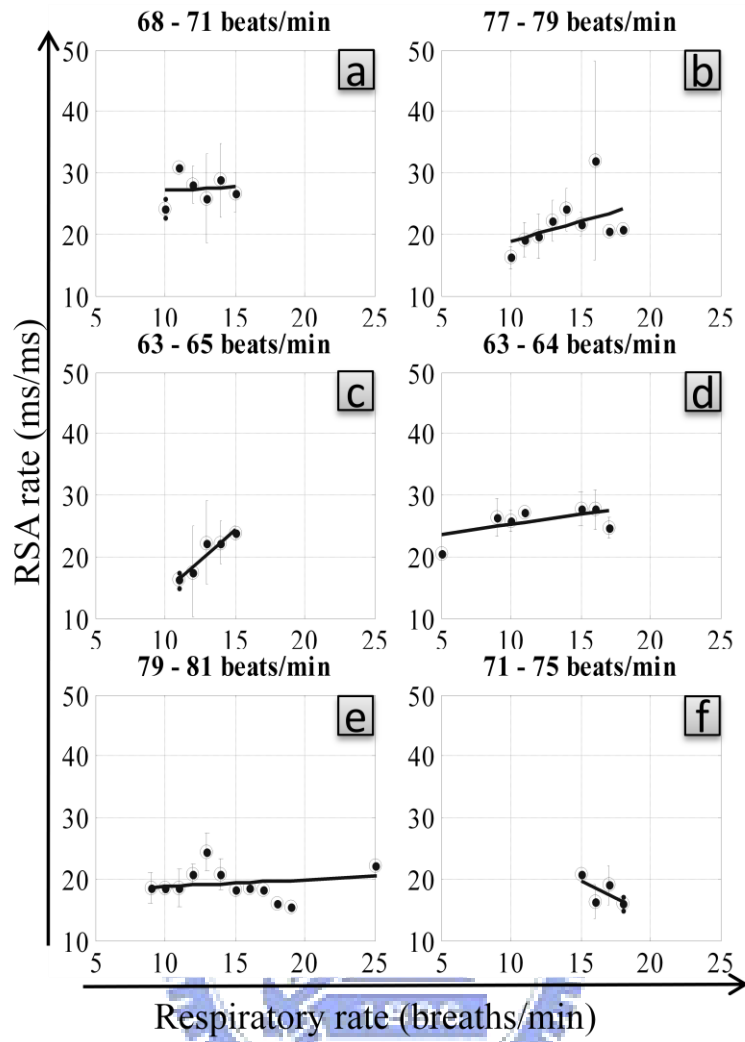


Fig.4. 7 RSA rate versus RR in the medium-HR range for experimental subject 1-6 (from (a) to (f)) during the first meditation session.

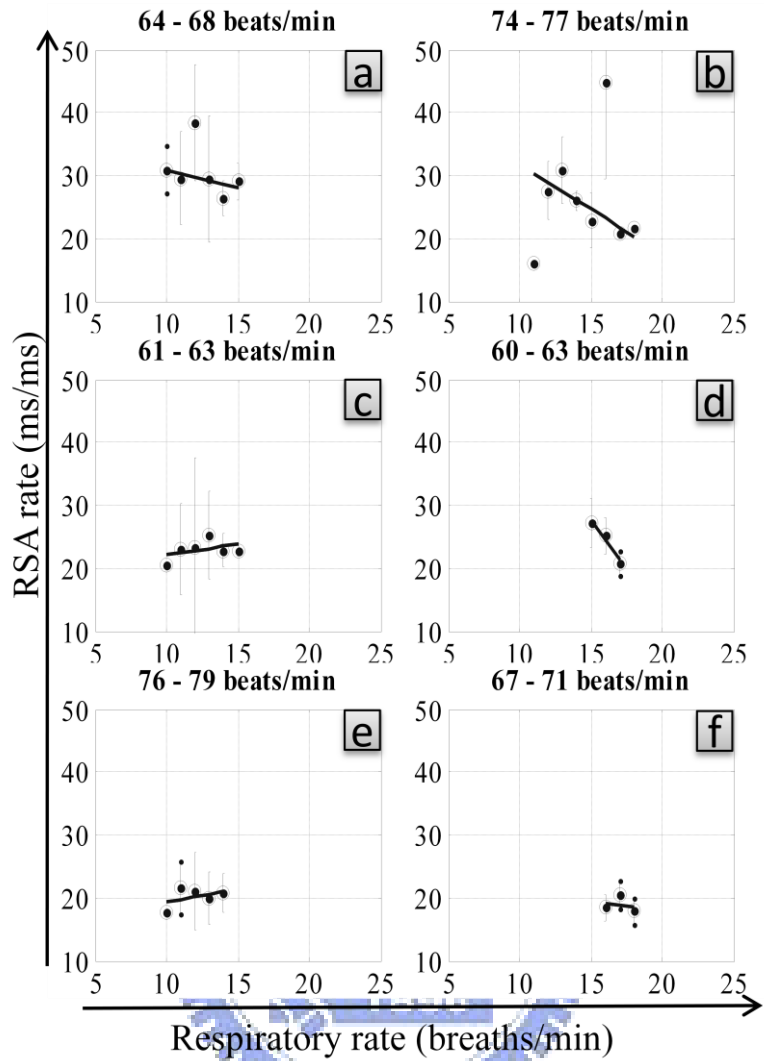


Fig.4. 8 RSA rate versus RR in the slow HR range for experimental subject 1-6 (from (a) to (f)) during the first meditation session.

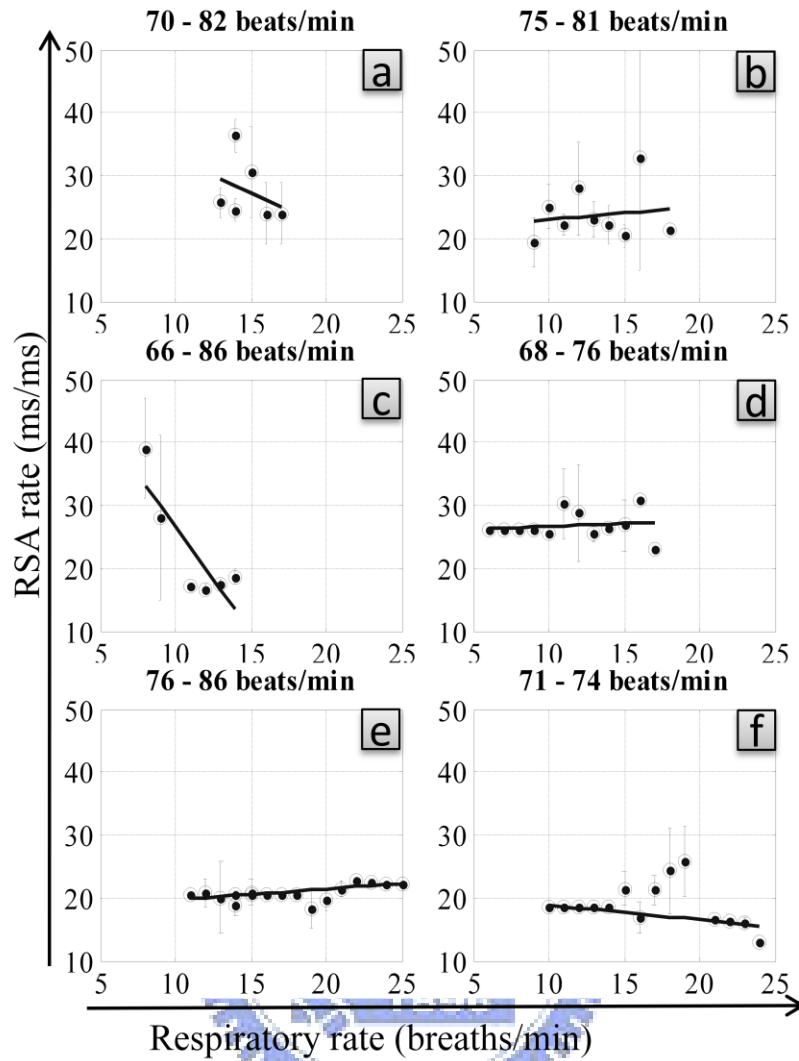


Fig.4. 9 RSA rate versus RR in the fast HR range for experimental subject 1-6 (from (a) to (f)) during the second meditation session.

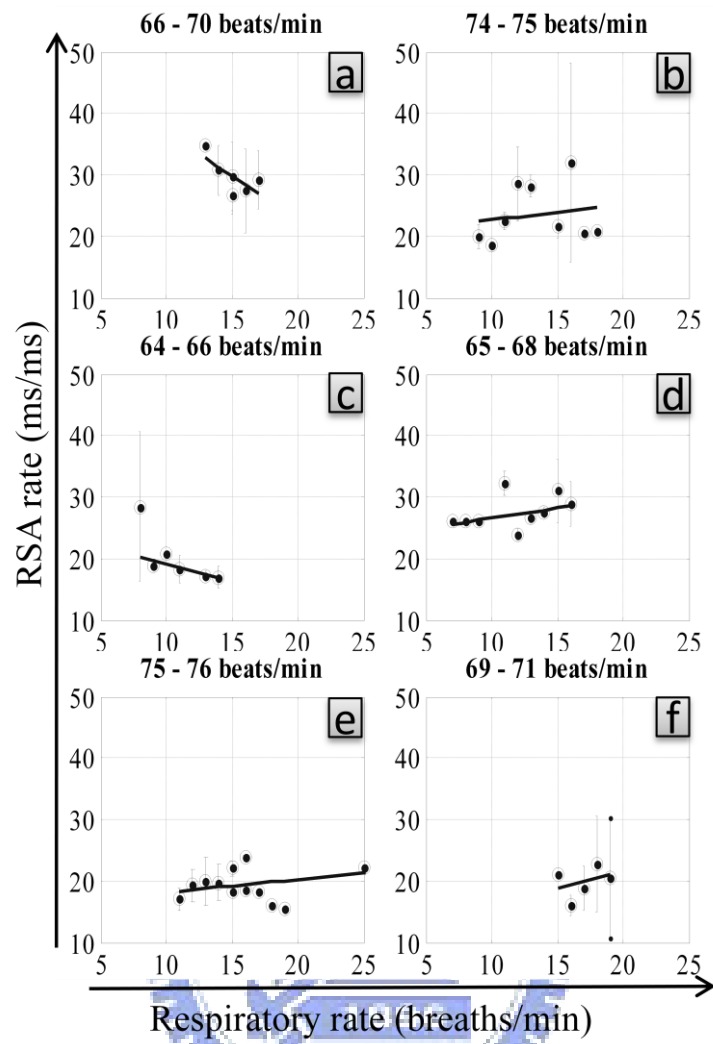


Fig.4. 10 RSA rate versus RR in the medium-HR range for experimental subject 1-6 (from (a) to (f)) during the second meditation session.

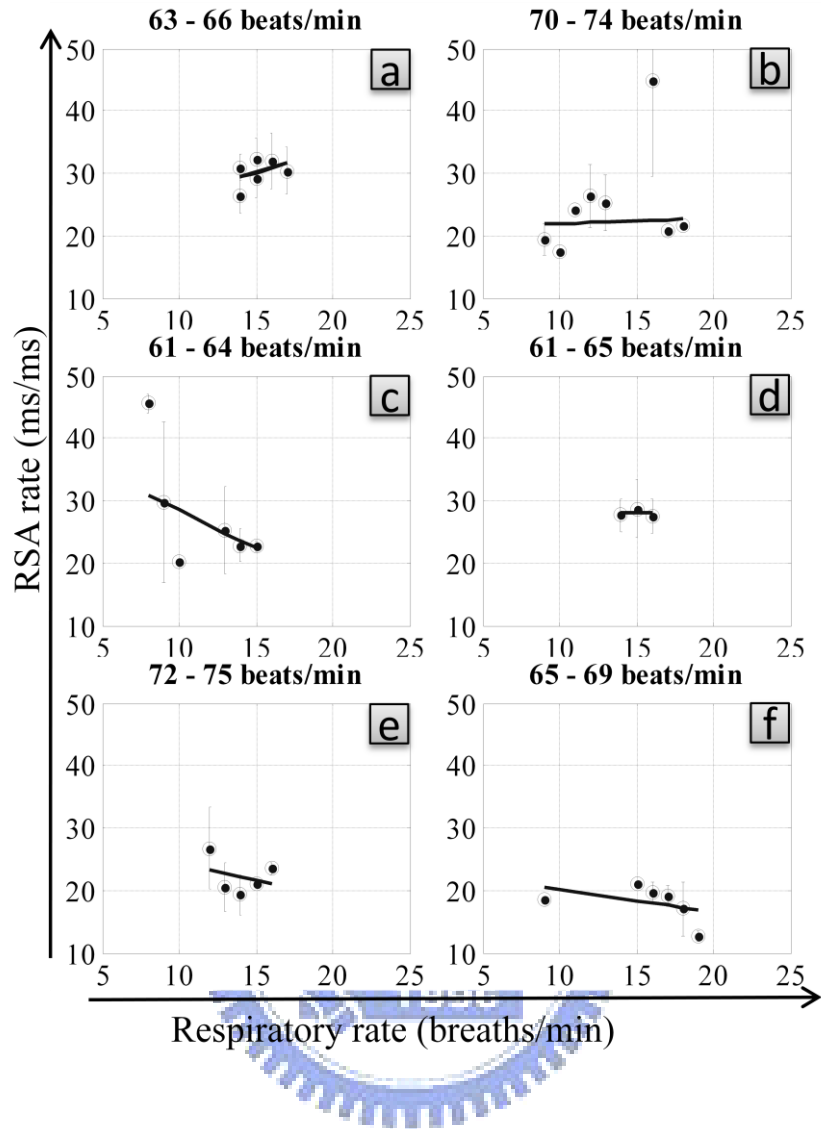


Fig.4. 11 RSA rate versus RR in the slow HR range for experimental subject 1-6 (from (a) to (f)) during the second meditation session.

Next, the slopes of each linear-regression lines in Figs 4.4-4.12 are computed and illustrated with the bar chart in Figs 4.13 (control group), 4.14 (experimental group, 1st meditation), and 4.15 (experimental group, 2nd meditation). The bar-chart illustration evidently verifies our interpretation on Figs 4.4-4.12. Apparently, most bars point downwards in Fig 4.14, reflecting negative correlation observed for control group.

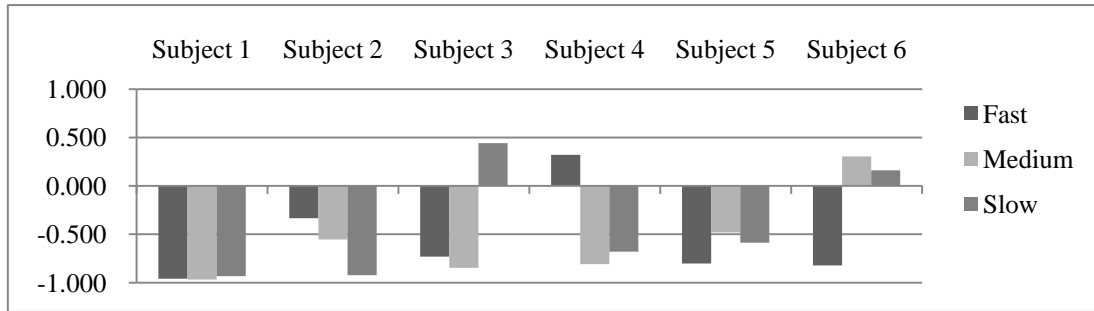


Fig.4. 12 Correlation coefficients of each individual control subject in the fast, medium and slow HR range.

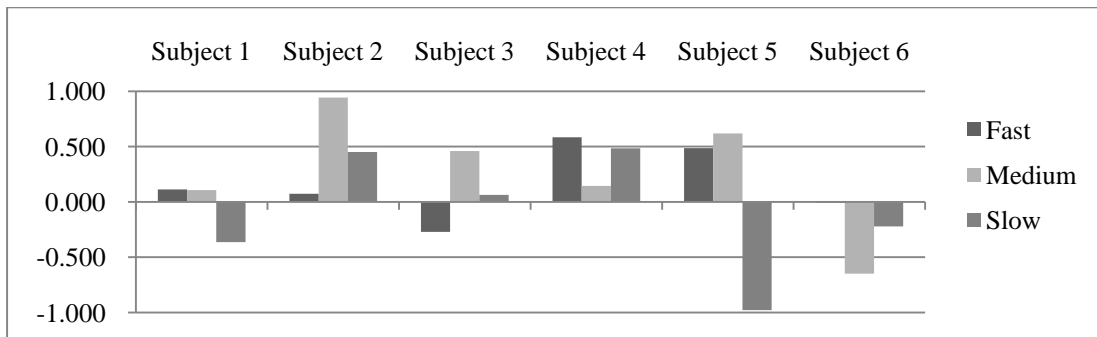


Fig.4. 13 Correlation coefficients of each individual experimental subject in the fast, medium and slow HR range during the first meditation session.

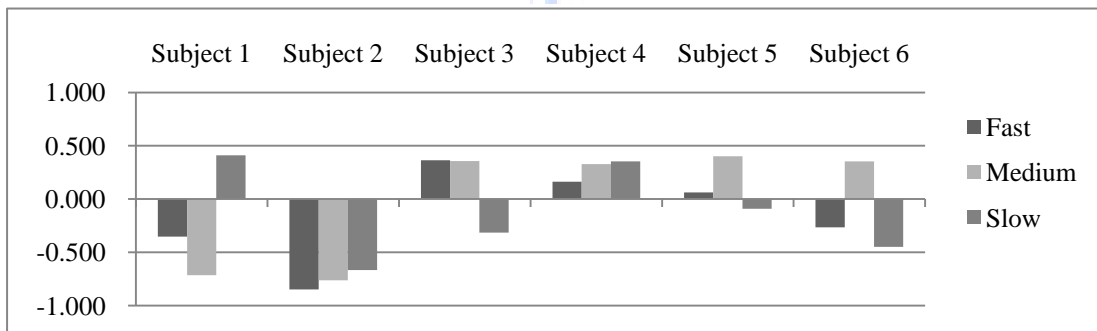


Fig.4. 14 Correlation coefficients of each individual experimental subject in the fast, medium and slow HR range during the second meditation session.

4.2.2 Results for entire group

In this section, we attempt to make a comparison between two groups by way of aggregating 30-minute data of all the subjects within the same group and following the same procedure as described in Section 4.2.1. That is, we first sort the entire data in descending HR order and then equally divide the R_{RSA} -versus-RR samples into 3 groups corresponding to fast, medium and slow HR.

The R_{RSA} -versus-RR samples for control group are plotted in Fig 4.16(a) for fast HR, 4.16(c) for medium HR, and 4.16(e) for slow HR. The R_{RSA} -versus-RR samples for experimental group are plotted in Fig 4.16(b) for fast HR, 4.16(d) for medium HR, and 4.16(f) for slow HR. HR range of experimental group (61-87 bpm) is 7 bpm lower than that of control group (68-94 bpm). RR values are more focalized for experimental group (8-18 breaths/min). Due to the breathing control protocol, the slowest breathing of control group extends toward 5 breaths/min, while the fastest breathing of 20 breaths/min reaches the upper bound of normal, resting breathing rate. Another noticeable aspect is the wider range of RSA rate in the control group, particular, in the group of slow HR.

We have noticed that there actually exist nonlinear correlation between RSA rate and RR. For simplification, we fit the data with multiple piecewise linear segments by dividing the RR ranges into one to three segments (Seg 1, Seg 2, and Seg 3), as listed in Table 4.2.

Table.4. 2 Multiple piecewise linear fitting for the correlation analysis between RSA rate and RR for control and experimental group in fast, medium and slow HR.

	Control group			Experimental group		
	Seg 1	Seg 2	Seg 3	Seg 1	Seg 2	Seg 3
Fast HR	5-10 (-)	10-20 (+)		8-10 (+)	10-18 (ϕ)	
Mid HR	5-10 (-)	10-15 (+)	15-20 (+)	8-10 (-)	10-16 (+)	16-18 (-)
Slow HR	5-10 (-)	10-20 (+)		9-17 (+)		

The notations (+), (-) and (ϕ) indicate positive, negative and null correlation, respectively. Apparently, we observe mostly negative correlation in the lower RR range (Seg 1) with respiration no faster than 10 breaths/min. On the contrary, medium respiration rates (in Seg 2) mostly result in positive correlation between RSA rate and RR.

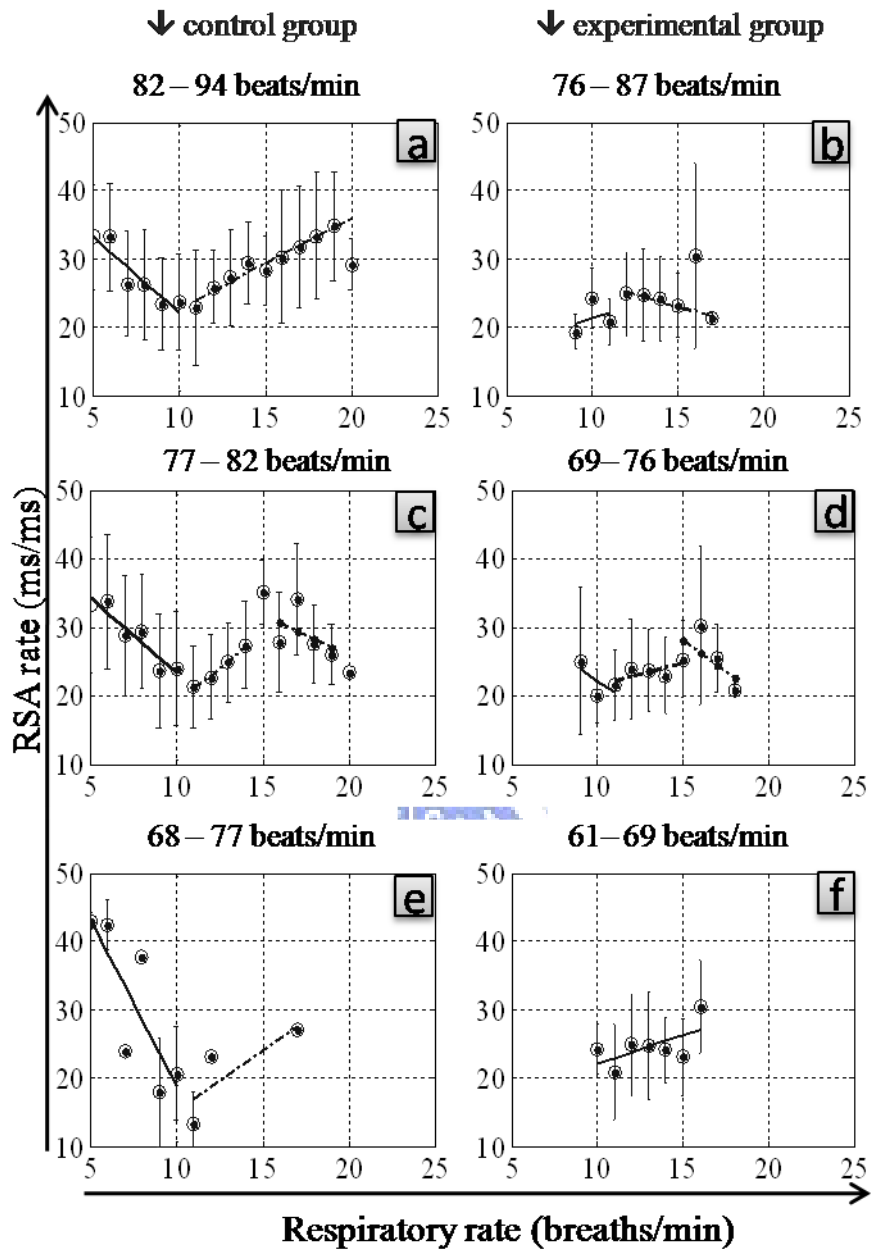


Fig.4. 15 Correlation analysis for RSA rate and RR based on the entire aggregating group data. Results of control group are plotted in (a) fast HR, (c) medium HR, and (e) slow HR. Results of experimental group are shown in (b) fast HR, (d) medium HR, and (f) slow HR.

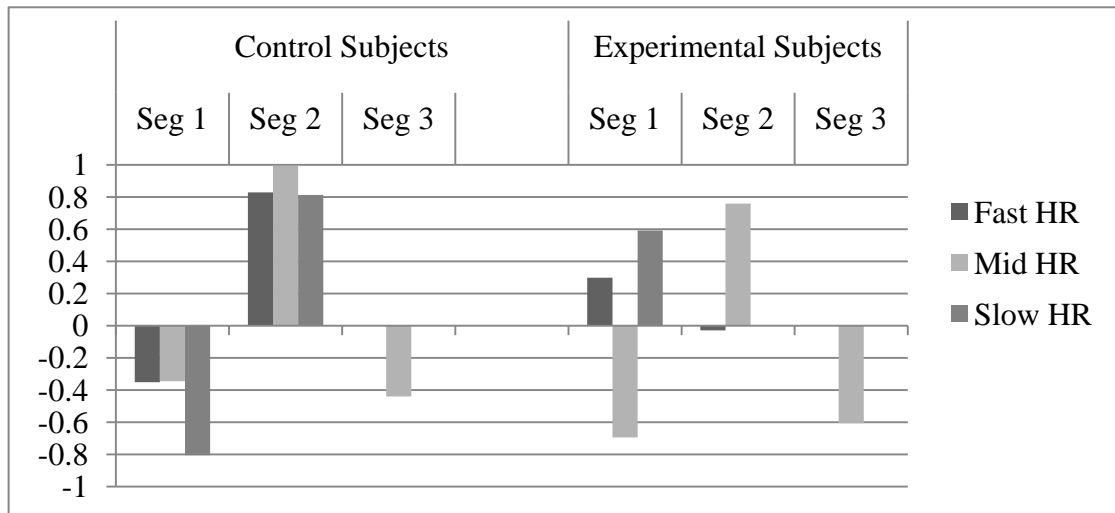
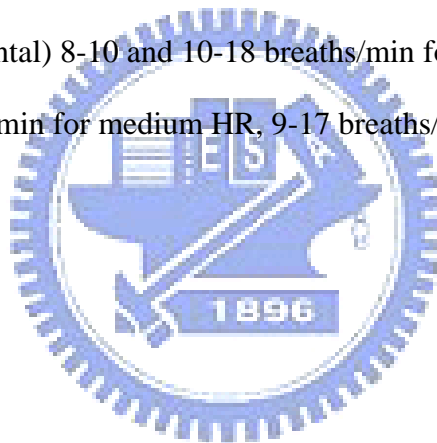


Fig.4. 16 Piecewise linear fitting: (control) 5-10 and 10-20 breaths/min for both fast and slow HR; 5-10, 10-15, and 15-20 breaths/min for medium HR.(experimental) 8-10 and 10-18 breaths/min for fast HR, 8-10,10-16, and 16-18 breaths/min for medium HR, 9-17 breaths/min for slow HR.



Chapter 5

Discussion and conclusion

5.1 Discussion and conclusion

This thesis reports our study on the phenomena of respiratory sinus arrhythmia (RSA) disclosed in the cardiorespiratory interaction. RSA can be used as an index of the efficiency of pulmonary gas exchange [9]. On the ECG waveform pattern, this phenomenon is characterized by the subtle change of R-R interval synchronizing with respiration. The main aim of this research was to investigate the effects of slow breathing on the RSA behaviors for both the experimental group (meditation practitioners) and control group (normal subjects without meditation experience).

According to the implementation strategy described in Chapter 3, there will be approximately 100 R_{RSA} samples in Section II and 60 R_{RSA} samples in Section III, with window size of 5 breathing cycles and moving step of 1 breathing cycle. Results of six control subjects all demonstrate the increase of RSA from Session II to III. By employing SPSS to the RSA rates, we may conclude the statistically significant difference between Sessions II and III ($p < 0.05$). Our preliminary results of control subjects mainly present the effect of breathing regulation on RSA behavior. It was found that breathing rate slowing down to 6 breaths per minute caused the significant influence on RSA rate.

In control group, most subjects exhibited negative relation between RSA rate and respiratory rate [22], that is, RSA rate increased with the slowing down of respiration. Whereas in the experimental group, we begin to observe some dominant positive correlation between RSA rate and respiratory rate in some practitioners. Such interesting contradiction between two groups arouses our attention. Based on our understanding of the core practice of *heart-purification* Chan meditation, practitioners often experience some halo-light energy surrounding the Heart Chakra during meditation. Such phenomenon might be the factor that speeds up the heart beating. Since Chan meditation mostly harmonizes the operation of different organ systems in the body, RSA rates might be maintained at a stable level. It appears that normal healthy subjects (control group) may well induce the RSA rate by slowing down respiration with constant breathing rate for a considerable duration. On the other hand, there still leave some uncertainties regarding the dependency of RSA rate on respiration for the Chan-meditation mechanism. These issues will be further investigated by appropriate experimental protocol in the future. Nevertheless, relationships disclosed in experimental group involved uncertainties that might be due to the intervention of other biological/conscious factors in meditation.

5.2 Future Work

Cardiorespiratory interactions exhibit complicated mechanisms that may involve the intervention from the other organ systems like the brain and nervous system. There leave a number of interesting issues to be studied in the future. For example, is RSA response directly regulated by respiration alone in meditation? Or, are RSA and respiration simultaneously regulated by the change of consciousness state of the *Chan-meditation* brain?

Reference

- [1] Sudsuang R., Chentanez V., Veluvan K. “Effect of buddhist meditation on serum cortisol and total protein levels, blood pressure, pulse rate, lung volume and reaction time,” *Physiology & Behavior*, vol. 50, 1991, pp. 543-548.
- [2] MacLean C.R.K., Walton K.G., Wenneberg S.R., Levitsky D.K., Mandarino J.P., Waziri R., Hillis S.L., Schneider R.H., “Effects of the transcendental meditation program on adaptive mechanisms: Changes in hormone levels and responses to stress after 4 months of practice,” *Psychoneuroendocrinology*, vol. 22, 1997, pp. 277-295.
- [3] Davidson R., Kabat-Zinn J., Schumacher J., Rosenkranz M., Muller D., Santorelli S., Urbanowski F., Harrington A., Bonus K., Sheridan J., “Alterations in brain and immune function produced by mindfulness meditation,” *Psychosom Med.*, vol. 65, Aug. 2003, pp. 564-570.
- [4] Lazar S., Kerr C., Wasserman R., Gray J., Greve D., Treadway M., McGarvey M., Quinn B., Dusek J., Benson H., Rauch S., Moore C., Fischl B., “Meditation experience is associated with increased cortical thickness,” *Neuroreport*, vol. 16, Nov. 2005, pp. 1893-1897.
- [5] Liu C.Y. and Lo P.C., “Investigation of spatial characteristics of meditation EEG using wavelet analysis and fuzzy classifier,” *Proceedings of the fifth IASTED International Conference: biomedical engineering*, 2007, pp. 91-96.

- [6] Huang H.Y. and Lo P.C., “EEG dynamics of experienced Zen meditation practitioners probed by complexity index and spectral measure,” *Journal of Medical Engineering & Technology*, vol. 33, May 2009, pp. 314-321.
- [7] Liu C.Y., Wei C.C., and Lo P.C., “Variation Analysis of Sphygmogram to Assess Cardiovascular System under Meditation,” *Evidence-Based Complementary and Alternative Medicine*, vol. 6, 2009, pp. 107-122.
- [8] Berntson G.G., Cacioppo J.T., and Quigley K.S., “Respiratory sinus arrhythmia: autonomic origins, physiological mechanisms, and psychophysiological implications,” *Psychophysiology*, vol. 30, Mar. 1993, pp. 183-196.
- [9] Giardino N.D., Glenny R.W., Borson S., and Chan L., “Respiratory sinus arrhythmia is associated with efficiency of pulmonary gas exchange in healthy humans,” *Am J Physiol Heart Circ Physiol*, vol. 284, May 2003, pp. H1585-1591.
- [10] Yasuma F. and Hayano J., “Respiratory Sinus Arrhythmia* Why Does the Heartbeat Synchronize With Respiratory Rhythm?,” *Chest*, vol. 126, Oct. 2004, pp. 1385-1386.
- [11] Peng C.K., Mietus J.E., Liu Y., Khalsa G., Douglas P.S., Benson H., and Goldberger A.L., “Exaggerated heart rate oscillations during two meditation techniques,” *International Journal of Cardiology*, vol. 70, Jul. 1999, pp. 101-107.
- [12] Yasuma F. and Hayano J., “Respiratory Sinus Arrhythmia*,” *Chest*, vol. 125,

2004, pp. 683-690.

[13] Bernardi L., Sleight P., Bandinelli G., Cencetti S., Fattorini L., Wdowczyk-Szulc J., and Lagi A., "Effect of rosary prayer and yoga mantras on autonomic cardiovascular rhythms: comparative study," *BMJ*, vol. 323, Dec. 2001, pp. 1446-1449.

[14] Goldschlager N., *Principles of Clinical Electrocardiography*, Appleton & Lange, 1989.

[15] Sahar T., Shalev A.Y., and Porges S.W., "Vagal modulation of responses to mental challenge in posttraumatic stress disorder," *Biological Psychiatry*, vol. 49, Apr. 2001, pp. 637-643.

[16] Doussard-Roosevelt J., Montgomery L., and Porges S., "Short-term stability of physiological measures in kindergarten children: Respiratory sinus arrhythmia, heart period, and cortisol," *Developmental Psychobiology*, vol. 43, Nov. 2003, pp. 230-242.

[17] Denver J.W., Reed S.F., and Porges S.W., "Methodological Issues in the Quantification of Respiratory Sinus Arrhythmia," *Biological psychology*, vol. 74, Feb. 2007, pp. 286-294.

[18] Grossman P., Stemmler G., and Meinhardt E., "Paced respiratory sinus arrhythmia as an index of cardiac parasympathetic tone during varying behavioral tasks" *Psychophysiology*, vol. 27, Jul. 1990, pp. 404-416.

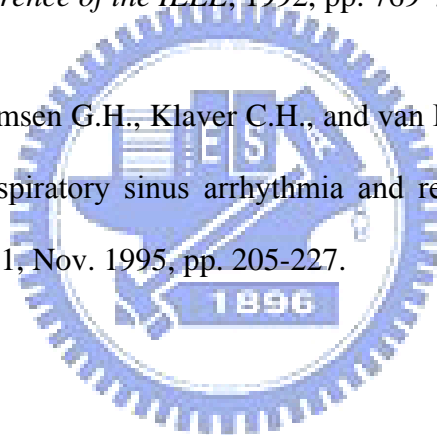
[19] Ritz T. and Dahme B., "Implementation and Interpretation of Respiratory Sinus

Arrhythmia Measures in Psychosomatic Medicine: Practice Against Better Evidence?,” *Psychosomatic Medicine*, vol. 68, 2006, pp. 617-627.

[20] Pfaltz M., Michael T., Grossman P., Peyk P., Margraf J., and Wilhelm F., “Ambulatory monitoring of respiration in panic disorder and posttraumatic stress disorder: Preliminary findings,” *Psychophysiology*, vol. 43, 2006, pp. S77-S77.

[21] Lopes P., Mitchell R., and White J., “The Relationships Between Respiratory Sinus Arrhythmia And Coronary Heart Disease Risk Factors,” *Engineering in Medicine and Biology Society, 1992. Vol.14. Proceedings of the Annual International Conference of the IEEE*, 1992, pp. 769-770.

[22] de Geus E.J., Willemsen G.H., Klaver C.H., and van Doornen L.J., “Ambulatory measurement of respiratory sinus arrhythmia and respiration rate,” *Biological Psychology*, vol. 41, Nov. 1995, pp. 205-227.



Appendix A

R Peak and Respiratory Peak Detections

A.1 R Peak Detection

The flow chart of R peak detection is shown in Fig. A.1. Original ECG signal that is digitized at 1000Hz is resampled to 200 Hz using Matlab's built-in polyphase filter implementation, including anti-aliasing (lowpass) FIR filter. Then the bandpass filter 10~30 Hz is used to reduce the influence of muscle noise, 60Hz interference, baseline drift, and T-wave interference. R peaks are strengthened by $x(n) * |x(n)|$. As shown in Fig. A.2, the ECG signal before and after preprocessing is presented, and the amplitude of R waves are obviously revealed. Because the amplitude of ECG signal is different from one to another, and there also exists difference amplitude for the same subject, thus the setting of a threshold must be adaptive so that R peak won't be missed or judged incorrectly. Therefore we use 1 minute moving window, and the threshold is determined by $0.3 * \text{maximum value in the window}$. From the above, we could detect the time position of R peak from ECG signal for further study.

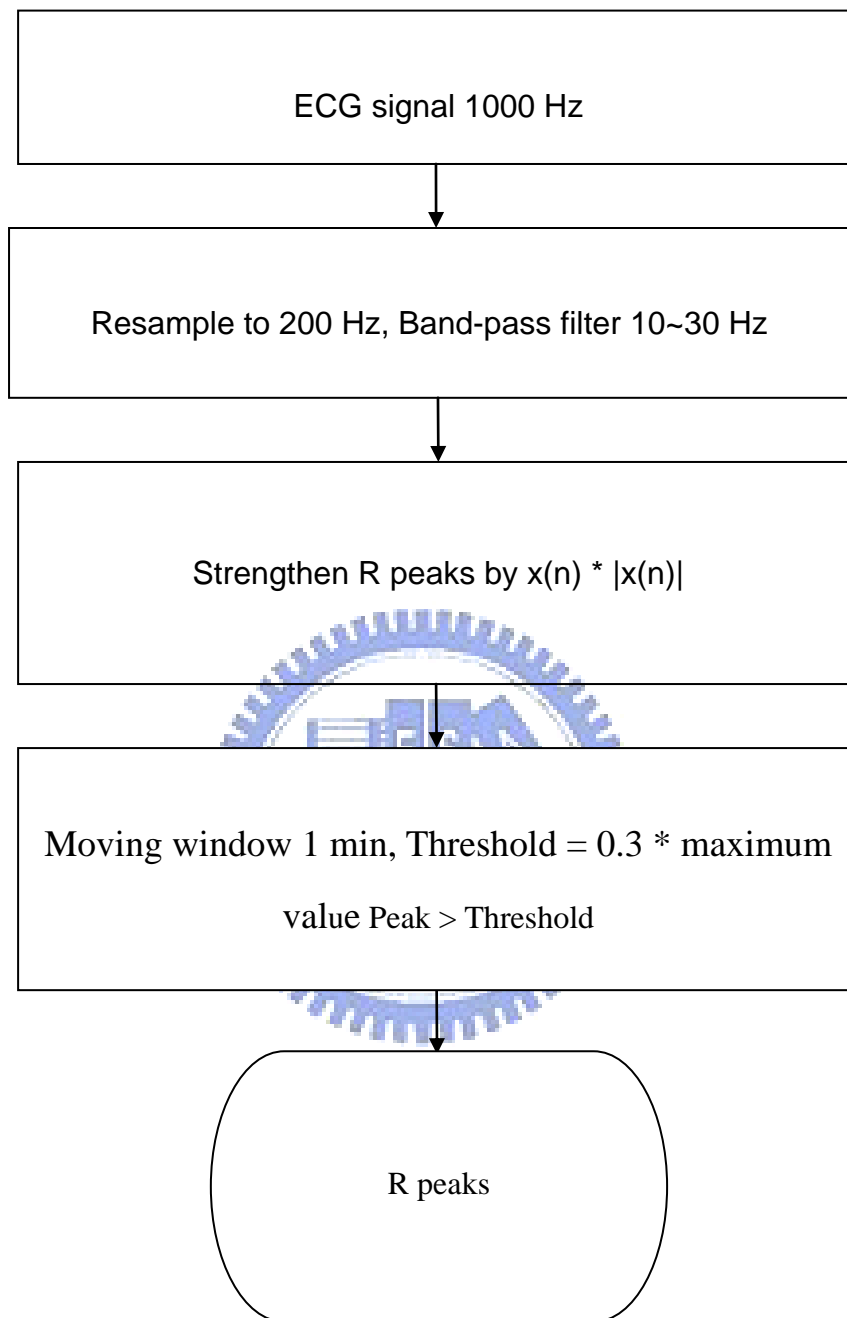


Fig.A. 1 Flow chart of R peak detection

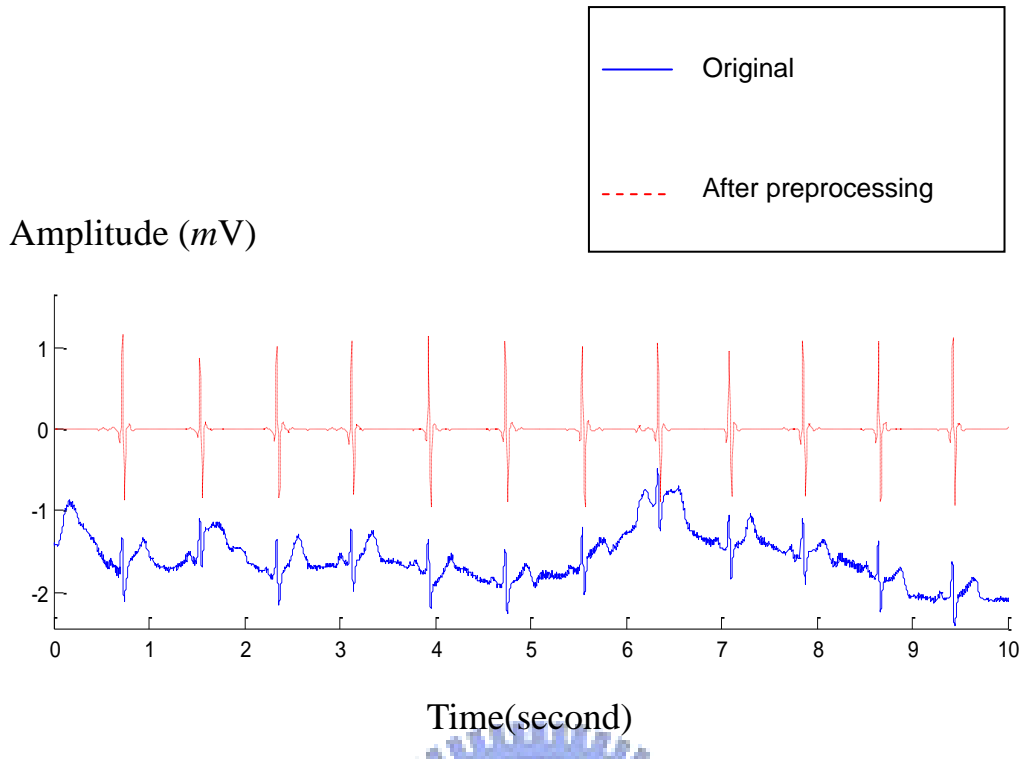


Fig.A. 2 ECG after preprocessing

A.2 Respiratory Peak Detection

The flow chart of Respiratory peak detection is shown in Fig. A.3. Original Respiratory signal that is digitized at 1000 Hz is resampled to 20 Hz using Matlab's built-in polyphase filter implementation, including anti-aliasing (lowpass) FIR filter. Then the bandpass filter 0.1~0.45 Hz is used to reducing the influence of baseline drift, and the main energy of respiratory signal is in this frequency range in this study. As shown in Fig. A.4, the respiratory signal before and after preprocessing is presented. In Fig. A.5, the parameters of normalized respiratory signal after preprocessing are shown, where t_k is the time position of k_{th} respiratory peak, d_{up} is the amplitude of inspiration, and d_{down} is the amplitude of expiration [78]. The conditions of d_{up} and $d_{down} > 0.05$ and the peak value at time $t_k > 0$ is considered to determine the

time position of respiratory signal for further study.

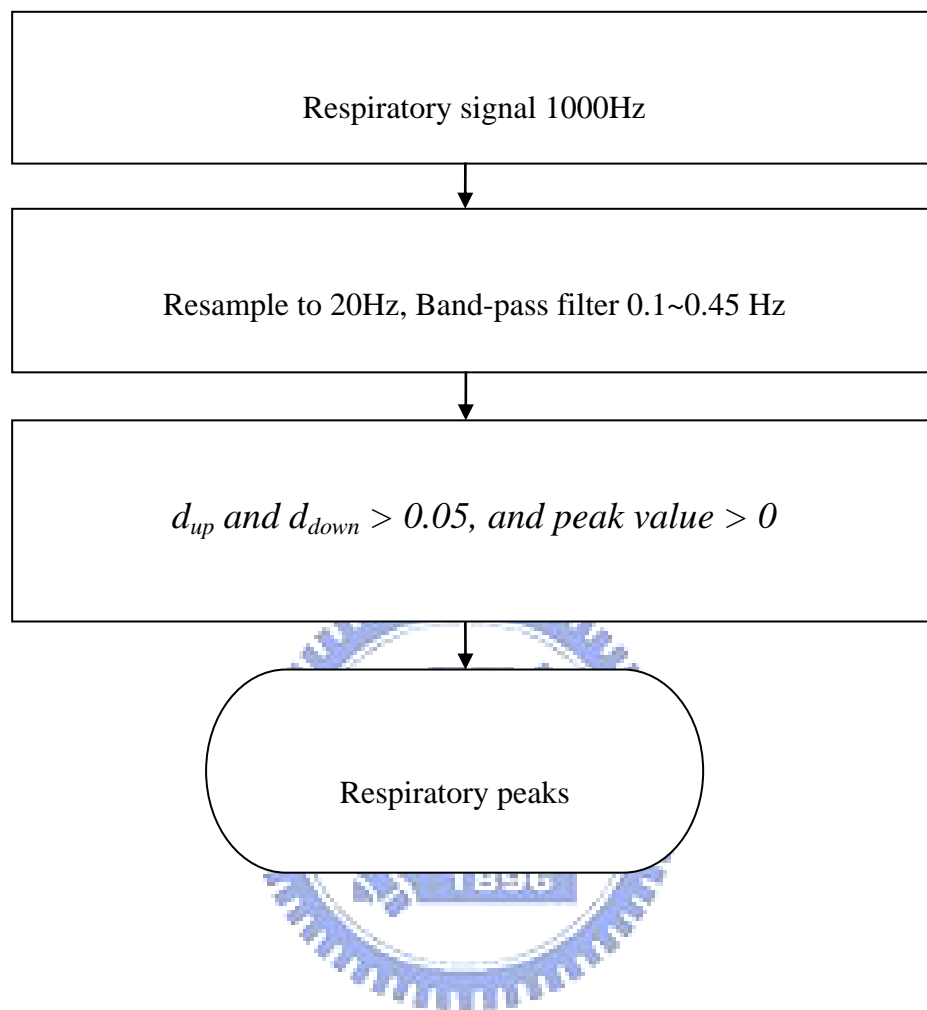


Fig.A. 3 Flow chart of Respiratory peak detection

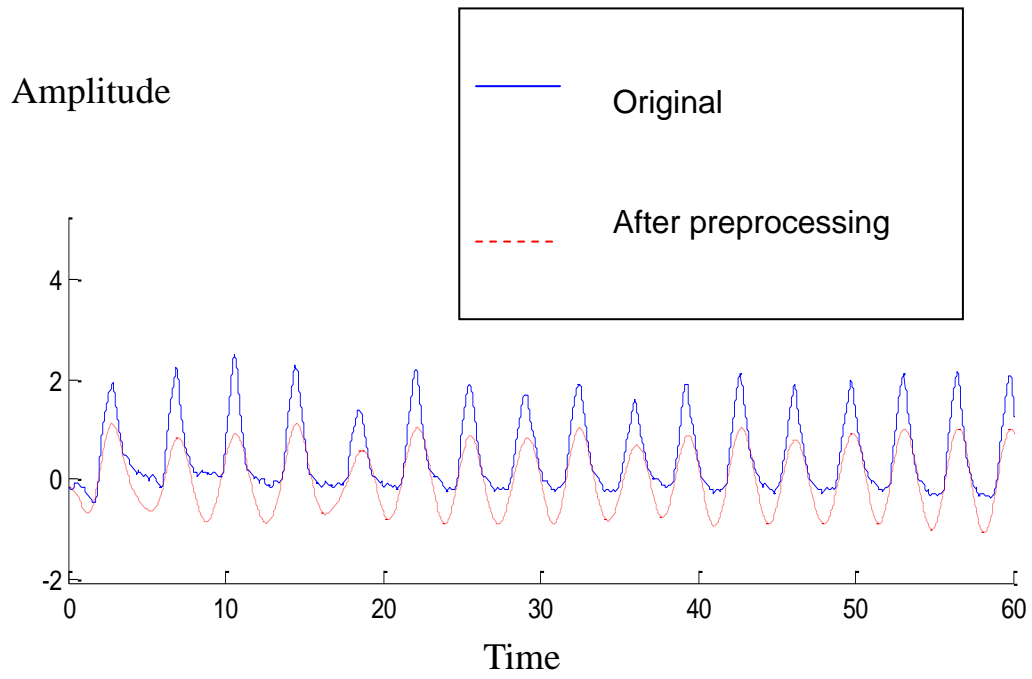


Fig.A. 4 Respiratory signal after preprocessing

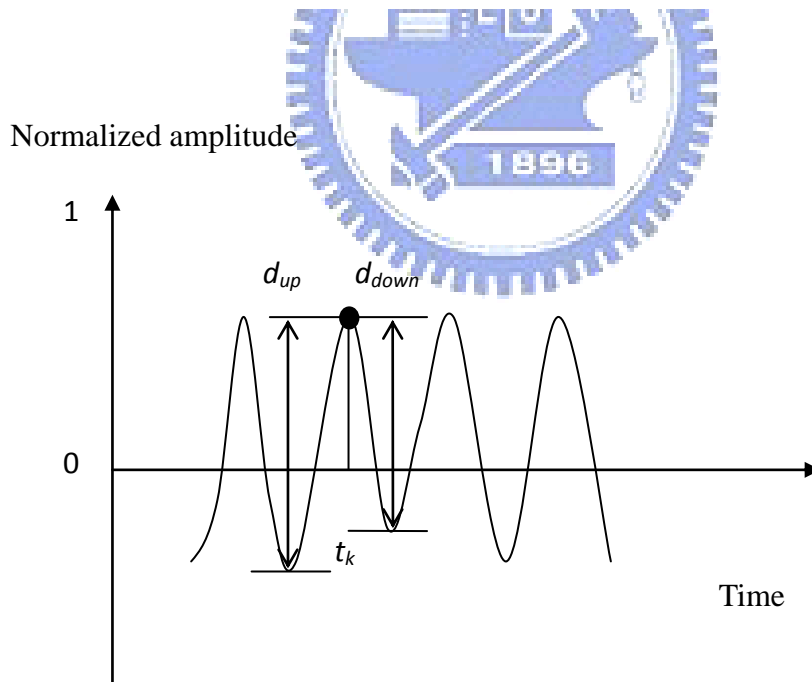


Fig.A. 5 The parameters of respiratory signal

Appendix B

Formal Chan-meditation Practice

Formal Chan-meditation course normally begins with a brief, solemn ritual called 開經偈 signifying “the opening ceremony of the practice towards complete enlightenment.” In the next 5-10 minutes, the class supervisor (normally, the experienced practitioner) shares wisdom words preached by the enlightened Chan Master, Wu Chueh Miao Tien, the 85th patriarch of orthodox Dharma-Chan sect. Meanwhile, practitioners sit calmly with meditation posture and belly breathing, yet, eyes opening.

Then, formal Chan-meditation session begins. In the beginning meditation, practitioners focus on particular chakras to activate the intrinsic potency and wisdom of those chakras. Gradually, the entire body-mind-spirit enters into a field of harmony after transcending the physical, mental, emotional and conscious realm. The goal of Chan meditation is to realize the *True Self* with eternal wisdom.

After the meditation session, practitioners open eyes and listen to the sharing from the supervisor for about ten more minutes. Then, the class ends with a brief closing ritual and the chanting of *The Song of True Self*.